vinyl alcohol and 3 mg/ml bovine serum albumin (BSA) [10]. Drops of the culture medium were covered with mineral oil (Nacalai, Tokyo, Japan) and maintained under 5% CO_2 in air at 37°C. Oocyte handling and micromanipulation were carried out in BSA-free Hepes-buffered KSOM medium (Hepes-KSOM; pH 7.4) in air.

Preparation of Oocytes and Cumulus Cells

B6D2F1(C57BL/6 × DBA/2) female mice (SLC, Shizuoka, Japan), 8–12 weeks of age, were used for the collection of recipient oocytes and donor cumulus cells. The mice were superovulated by the injection of 7.5 IU eCG, followed by 7.5 IU hCG about 48 h later. Oocytes were collected from the oviducts about 15 h after hCG injection and released from the cumulus cells by treatment with 0.1% bovine testicular hyaluronidase in KSOM medium. These oocytes and cumulus cells were incubated in KSOM until use. All procedures described within were reviewed and approved by the Animal Experimental Committee at the RIKEN Institute and were performed in accordance with the Guiding Principles for the Care and Use of Laboratory Animals.

Nuclear Transfer and Oocyte Activation

Nuclear transfer and oocyte activation were carried out according to the method reported previously [11, 12]. The timing of NT and oocyte activation differed according to the experimental groups, as described below. The recipient MII oocytes were enucleated, together with a small amount of the surrounding cytoplasm in Hepes-buffered KSOM that contained 7.5 μg/ml cytochalasin B (Calbiochem, Darmstadt, Germany) on a heated manipulation stage (37°C). Enucleation was performed using a Piezo-driven micromanipulator (Prime Tech, Ibaraki, Japan). The oocytes were allowed to regenerate their membranes in KSOM medium for 1–2 h. For NT, the cumulus cells were placed in 6% polyvinylpyrrolidone solution, and their nuclei were injected into enucleated oocytes in Hepes-buffered KSOM at room temperature using the Piezo-driven micromanipulator. The oocytes were activated by treatment with 3 mM $SrCl_2$ in Ca^{2+}-free KSOM medium for 1 h. When NT was carried out before oocyte activation (standard protocol, Group A), the oocytes were cultured for an additional 5 h in the presence of 5 μg/ml cytochalasin B to prevent the extrusion of a polar body that contained some of the donor chromosomes.

Experimental Design

This study involved five experimental groups (Fig. 1): Group A, standard NT protocol, in which the oocytes were activated 2 h after NT; Group B, simultaneous NT, in which the oocytes were activated within 5 min after NT; Group C, delayed NT, whereby NT was performed 2 h after activation; Group D, diploid parthenotes, in which the oocytes were activated without enucleation and NT; and Group E, enucleated oocytes, whereby the oocytes were enucleated and activated without NT. The distribution patterns of the microtubules, microfilaments, and chromosomes were observed at 2, 8–12, and 15 h after activation using the indirect immunofluorescence method described below.

Some of the delayed NT oocytes were treated with Taxol, which promotes microtubule assembly, to investigate whether microtubule network reformation improved the abnormal cellular kinetics of delayed NT oocytes. In a preliminary experiment using parthenogenetic embryos, we found that Taxol treatment itself induced abnormal, uneven cleavage or mild fragmentation (consisting of two to eight fragments) of embryos. Therefore, we employed two protocols in which embryos were subjected to long- or short-term exposure to Taxol-containing medium. In the first protocol, enucleated oocytes were activated for 1 h with $SrCl_2$ in Ca^{2+}-free KSOM medium that contained 1.5 μM Taxol. After 1 h of treatment with Taxol in normal KSOM medium and nuclear transfer, the reconstructed oocytes were treated with Taxol for a further 1–2 h (total of 3–4 h exposure to Taxol). In the second protocol, delayed NT oocytes, which were prepared as described above (Group C), were exposed to 0.2 μM Taxol for only 10 min after nuclear transfer. In both protocols, the reconstructed oocytes were cultured in Taxol-free KSOM for 72 h, and their developmental stages were recorded.

Immunofluorescence Staining

Oocytes were fixed and immunostained for microtubules, microfilaments, and DNA using a modification of the method described by Navara et al. [9]. Briefly, zona pellucidae were removed with acidified M2 medium (pH 2.5) at 37°C. After a 30-min period of recovery at 37°C, the zona-free oocytes were attached to MAS-coated slide glasses (Matsunami

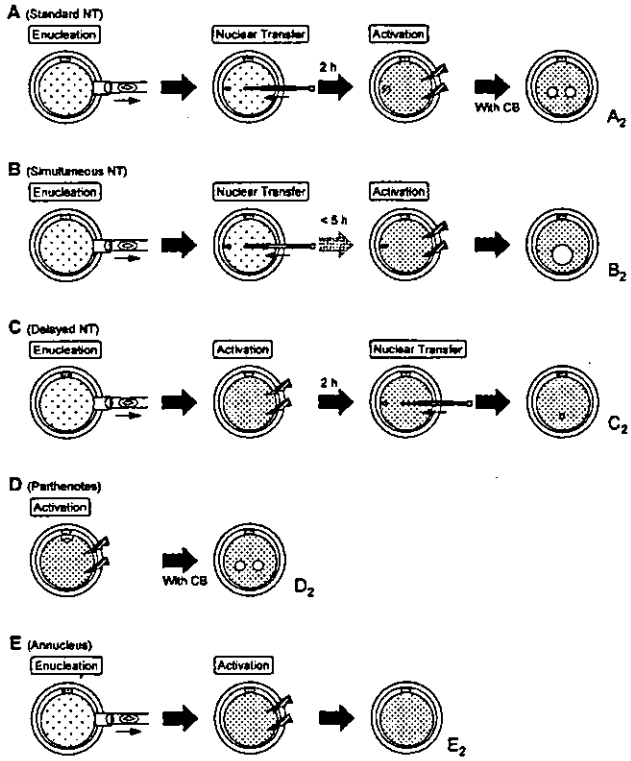

FIG. 1. Scheme showing the experimental groups. Nuclear transfer was undertaken with three different time schedules (Groups A–C). Groups D and E are non-NT groups. The characters A_2–E_2 correspond to those used in Figure 3.

Glass, Tokyo, Japan) and extracted for 2–3 min with buffer M (25% [v/v] glycerol, 50 mM KCl, 0.5 mM $MgCl_2$, 0.1 mM EDTA, 1 mM EGTA, 50 mM imidazole hydrochloride, and 1 mM 2-mercaptoethanol; pH 6.8) that contained 0.01%–0.2% Triton X-100. The permeabilized oocytes were transferred to dry slide glasses and fixed in 3% formaldehyde for 20 min at room temperature. Permeabilization and fixation were performed at 37°C to maintain the original microtubule configuration. Fixed oocytes were then blocked overnight with 0.1 M PBS that contained 0.1% Triton X-100 and 3 mg/ml BSA (PBS-TX-BSA) at 4°C. The oocytes were incubated with a murine monoclonal antibody against α-tubulin (clone DM 1A, diluted 1:500; Sigma Chemical Co., St. Louis, MO) for 40 min at 37°C. After washing in PBS-TX-BSA, the samples were stained with FITC-conjugated goat anti-mouse IgG antibody (diluted 1:100; Sigma). They were then nuclear stained for DNA with DAPI (4,6-diamidino-2-phenylindole) or propidium iodide. For the staining of actin filaments, the oocytes were cultured with rhodamine-conjugated phalloidin (50 μg/ml; Sigma) before DNA staining. The slide glasses were mounted in antifade medium (Vectashield; Vector Labs, Burlingame, CA) and examined using a TE2000 epifluorescence microscope (Nikon, Tokyo, Japan).

RESULTS

In this study, 5–30 oocytes were observed immunohistochemically for each group at each time point. The results from at least two replicate experiments are summarized. The localization patterns of the microtubules and chromosomes were essentially the same within a set of oocytes, except for those observed at 8–12 h in Groups C and E, which consisted of various misshapen forms before fragmentation.

Behavior of Cytoplasmic Asters in Nuclear-transferred MII Oocytes

We examined the behavioral patterns of the cytoplasmic asters in MII-arrested oocytes, both before and after NT.

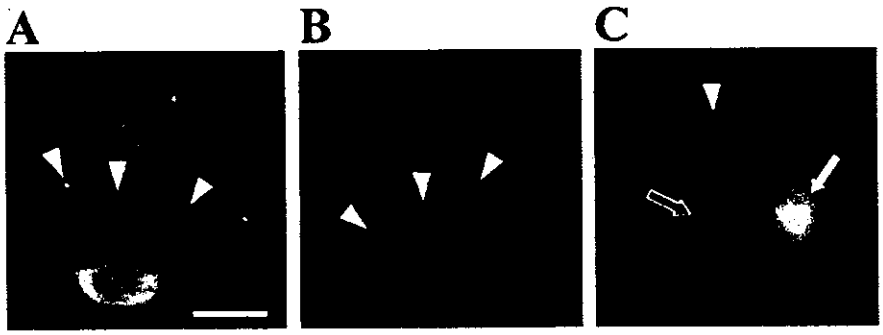

FIG. 2. Cytoplasmic asters in MII oocytes before and after NT. A) Intact MII oocytes, which contain an average of approximately 15 asters per oocyte (arrowheads; see text for details). B) MII oocytes after enucleation. No change is found in the number or distribution of asters (arrowheads) as compared with intact oocytes. C) Enucleated oocytes 1 h after NT. The number of cytoplasmic asters (arrowhead) is decreased significantly, whereas a newly formed spindle encloses the condensed donor chromosomes (white arrow). The area proximal to the spindle contains fewer asters (black arrow) than the area distal to the spindle. Bar = 20 μm.

Removal of the meiotic spindles from MII oocytes did not change the number or distribution of cytoplasmic asters (14.9 ± 3.0 vs. 15.1 ± 3.8 (mean ± SD asters per oocyte; $P > 0.05$; Fig. 2, A and B). However, 1–2 h after transfer of the donor nucleus, the number of cytoplasmic asters decreased significantly (8.9 ± 2.9; $P < 0.01$), whereas a newly formed spindle enclosed the condensed donor chromosomes (Fig. 2C). The area proximal to the spindle had fewer asters than the area distal to the spindle (Fig. 2C). These findings suggest that cytoplasmic asters participate in the reformation of the metaphase spindle that anchors the donor chromosomes.

Behavior of Microtubules in Nuclear-transferred Oocytes After Activation

To gain a better understanding of the postactivation behavior of microtubules in nuclear-transferred oocytes, we observed the temporal and spatial changes in microtubule distribution in the oocytes from three groups with different NT and activation timings (see Fig. 1 for experimental design). At 1–2 h after activation (Fig. 3, A_1, B_1, and C_1), the oocytes proceeded to the anaphase-telophase transition. At this stage, cytoplasmic asters were undetectable in Groups A and C, whereas some asters were detected in Group B. Although the asters that had exhibited intense fluorescence disappeared, the fine microtubule network remained and was evenly distributed throughout the cytoplasm. Intense fluorescence for tubulin was restricted to the spindle between the segregating donor chromosomes in Group A (standard NT; Fig. $3A_1$). When the chromosomes segregated into three masses, a tridirectional spindle was formed (Fig. $3A_1$, inset). In Group B (simultaneous NT), dense bundles of microtubules (or assemblies of asters) often surrounded the introduced donor nucleus (Fig. $3B_1$).

At 8–12 h after activation (Fig. 3, A_2, B_2, and C_2), the oocytes were at the midpronuclear stage and formed two pseudopronuclei (Group A) or one large pseudonucleus (Group B). The spindle-shaped dense microtubule arrays were still found between the two pseudopronuclei in Group A. In Group C oocytes (delayed NT), the donor nucleus retained its original size or was slightly larger, and strong fluorescence was absent in the cytoplasm or around the nucleus. The fine microtubule network was present in the cytoplasm, although its distribution was very irregular. Many of these delayed NT oocytes had bumpy surfaces and showed irregular distributions of microfilaments and microtubules within the ooplasm (Fig. 4B). This finding is in marked contrast to the observations of oocytes from Group A, in which the microfilaments were evenly distributed only on the surface area of the cortex (Fig. 4A).

At 15 h after activation (Fig. 3, A_3 and B_3), most of the oocytes in Groups A and B entered the prometaphase or metaphase, as evidenced by nuclear membrane breakdown. All of the oocytes in Group C showed complete fragmentation at this stage (see also Fig. 5). During the early prometaphase, the condensing chromosomes were surrounded by dense microtubule arrays without nucleation sites, whereas several asters reappeared in the cytoplasm (Fig. $3A_3$). As this stage proceeded, the asters migrated to the condensed chromosomes and gradually formed the mitotic spindle. This type of microtubule behavior was common to Groups A and B.

In the non-NT oocytes (Groups D and E), the chromosomes and microtubules behaved as those in the NT groups (Groups A and C, respectively). The parthenogenetically activated oocytes in Group D (Fig. 3D) showed the same microtubule distribution pattern as those in Group A (Fig. 3A), although the chromosome composition of the (pseudo)pronuclei was different (in parthenogenetic oocytes, each pronucleus contained a haploid set of chromosomes). The oocytes in Group E were enucleated, but not nuclear-transferred (Fig. 3E). After activation, they underwent fragmentation within 15 h, in a similar fashion to the delayed NT oocytes in Group C (Fig. 3C).

In Groups A and D, the microfilament-disrupting agent cytochalasin was included in the medium for the first 6 h postactivation to prevent polar body extrusion. In preliminary experiments, we confirmed that this treatment had no significant effects on the behavioral patterns of the microtubules or cytoplasmic asters (data not shown).

TABLE 1. Effect of Taxol treatment on in vitro development of embryos reconstructed by delayed NT with cumulus cells.

	No. observed	No. (%) fragmentation	No. (%) 1-cell	No. (%) 2-cell	No. (%) 4-cell	No. (%) morula blasts.	No. (%) abnormal cleavage*
Taxol 3–4 h	110	0 (0.0)	0 (0.0)	0 (0.0)	0 (0.0)	0 (0.0)	110 (100.0)
Taxol 10 min	149	124 (83.2)	7 (4.7)	11 (7.4)	2 (1.3)	5 (3.4)	0 (0.0)
No treatment	78	78 (100.0)	0 (0.0)	0 (0.0)	0 (0.0)	0 (0.0)	0 (0.0)

* Including mild fragmentation induced by toxicity of taxol.

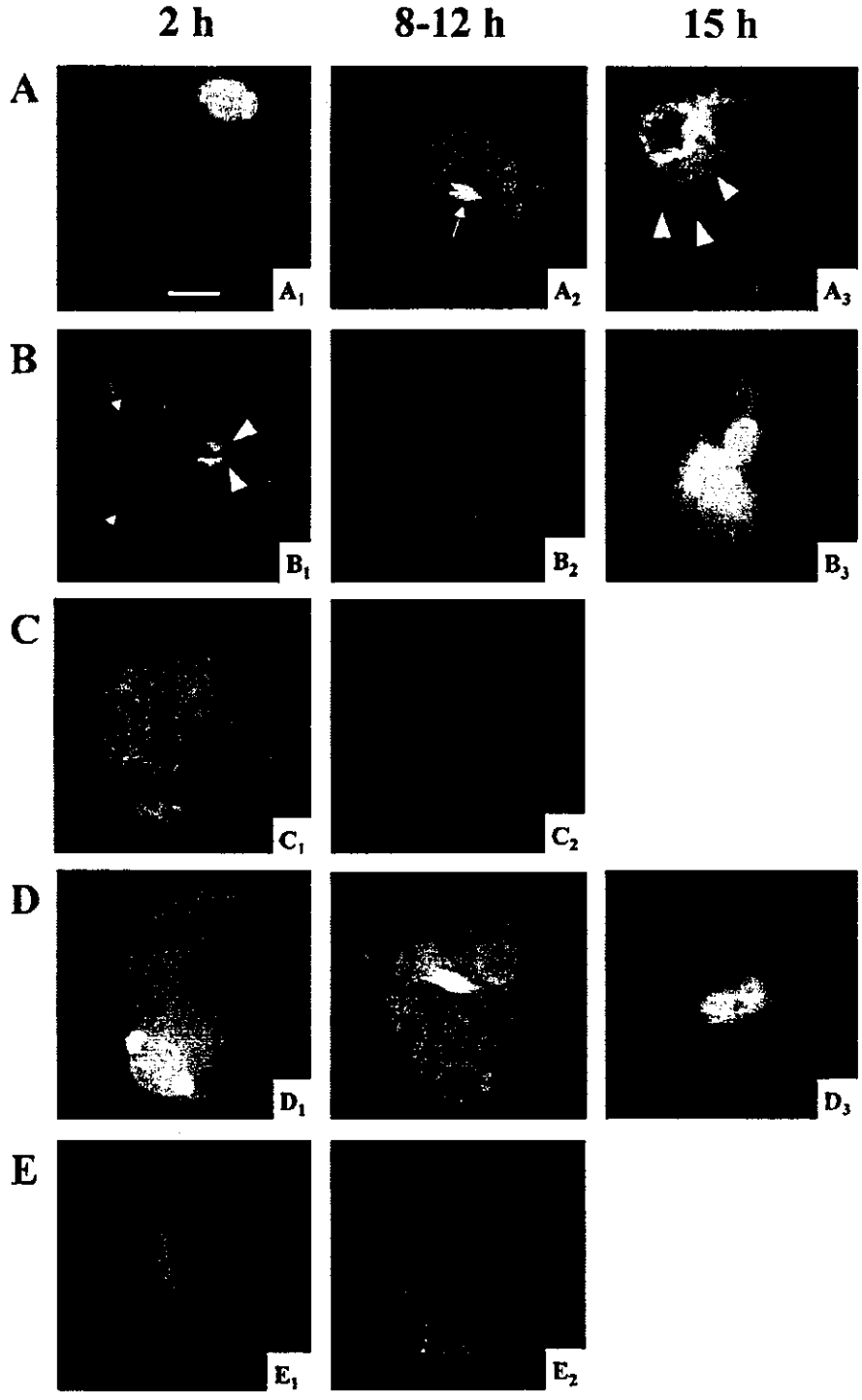

FIG. 3. Distribution of microtubules (green) and chromosomes (red or blue) in NT and parthenogenetic embryos after activation. A) Group A (standard NT). At 2 h after activation (A_1), the oocyte is in telophase II, and the donor chromosomes are segregated into two compact masses (red). The chromosomes rarely segregated into three masses (inset). Cytoplasmic asters are not visible. At 8–12 h (A_2) after activation, the pseudopronuclei (blue) are fully swollen. Intense staining for microtubules is seen in the remnant of the spindle (arrow), whereas a fine microtubule network is formed in the entire cytoplasm (see also Fig. 4A). At 15 h (A_3) postactivation, the nuclei show the prometaphase configuration with condensing chromosomes. Several asters (arrowheads) appear in the cytoplasm. B) Group B (simultaneous NT). At the stage corresponding to telophase II (2 h; B_1), the donor chromosomes are not segregated but are condensed in a single mass (red). Cytoplasmic asters persist in the cytoplasm (arrows) and around the donor nucleus (arrowheads). At 8–12 h (B_2), a large pseudopronucleus develops and asters are not present. The oocytes enter mitosis by 15 h (B_3) postactivation, as in Group A. This oocyte is already in the mitotic telophase. Microtubules are distributed mainly to the spindle and around the sister chromosomes. C) Group C (delayed NT). The donor nuclei are introduced into recipient oocytes 1–2 h after activation. The photo shows an enucleated oocyte before NT. It has no cytoplasmic asters (C_1). At 8–12 h (C_2), the donor nucleus retains its original size. Uneven distribution of the fine microtubule network is noted in the cytoplasm (see also Fig. 4B). By 15 h, all of the NT oocytes have undergone fragmentation (see Fig. 5C). D) Group D (diploid parthenote). The behavioral patterns of the microtubules and chromosomes are very similar to those in the standard NT group (A). The oocyte at 15 h (D_3) is in late prometaphase, showing completely condensed chromosomes (red) and dense microtubules (green) shortly before spindle formation. E) Group E (enucleated oocytes). The oocytes lack nuclei and have undergone fragmentation, as is seen for the oocytes in Group C. The irregular distribution pattern of fine microtubules (E_2) is very similar to that in Group C (C_2). Bar = 20 μm.

Effect of Taxol Treatment on the Behavior of Delayed NT Oocytes

The behavior of microtubules and microfilaments, as described above, indicates that cytoplasmic fragmentation in delayed NT oocytes (Group C) may be attributed to the absence of cytoplasmic asters at the time of NT. To obtain further experimental evidence to support this hypothesis, we treated recipient oocytes with Taxol, which is a microtubule-assembling agent, and examined whether the enhancement of microtubule assembly improved the cellular kinetics of these delayed NT oocytes. In the first protocol, numerous aster-like structures were found in the cytoplasm 2 h after Taxol treatment (shortly before NT), irrespective of the presence or absence of oocyte chromosomes (Fig. 5A). Taxol-treated oocytes were then reconstructed with the

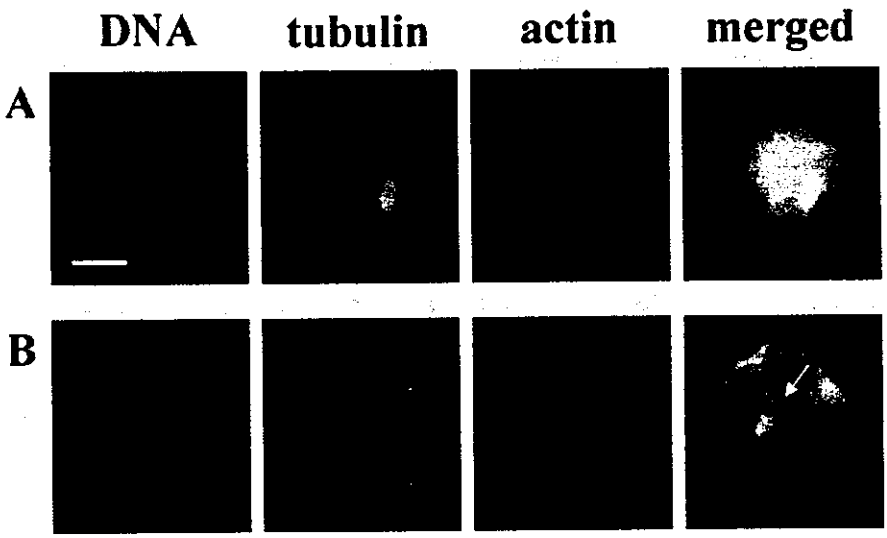

FIG. 4. Oocytes after standard NT or delayed NT, 8 h after activation. The oocytes were stained for the localization of nuclei (blue), microtubules (green), and microfilaments (red). An oocyte after standard NT in (A) has a regular round shape and shows even distributions of fine microtubules in the cytoplasm and of microfilaments in the cortex area. The arrow indicates the remnant of the spindle. In contrast, an oocyte that was subjected to delayed NT (B) has a bumpy surface and irregular distributions of microtubules and microfilaments. The dense yellow bundles in the merged photomicrograph indicate colocalization of microtubules and microfilaments in the cytoplasm (arrows). Bar = 20 μm.

donor nucleus that was produced by delayed NT and cultured for 15 h. As expected, the reconstructed oocytes did not show severe fragmentation that was specific for delayed NT, but did show uneven cleavage or mild fragmentation with two to eight karyoplasts/cytoplast (Fig. 5B). These oocytes showed arrested development thereafter (Table 1). In the second protocol, the oocytes were exposed to Taxol for only 10 min, immediately after nuclear transfer, to minimize the cytotoxic effect of Taxol. Although delayed NT-specific severe fragmentation was induced in some oocytes, the remaining oocytes (n = 25) survived the first cell cycle. Of the latter 25 oocytes, five (20%) developed to the morula/blastocyst stage (two morulae and three blastocysts; Fig. 5B, inset; Table 1). In contrast, all of the oocytes in the nontreated group underwent complete fragmentation (Fig. 5C).

DISCUSSION

It is generally accepted that the coordinated behavior of microtubules and donor chromosomes in nuclear-transferred oocytes is a prerequisite for the subsequent normal development of cloned embryos [13–15]. Murine MII oocytes contain two microtubule-containing structures: the meiotic spindles and a dozen cytoplasmic microtubules (asters). The meiotic spindles are crucial for the proper alignment and separation of the chromosomes during meiosis, whereas the cytoplasmic asters are responsible for pronuclear apposition following sperm incorporation [9]. The meiotic spindles are removed from MII oocytes before NT. In this report, we show that in the mouse, the cytoplasmic asters play key roles in pronuclear movement following oocyte activation and in donor chromosome alignment during spindle formation in recipient MII oocytes. The cytoplasmic asters in nuclear-transferred oocytes are probably assembled in the spindle poles, thereby stabilizing the spindle microtubules.

The situation described above is in sharp contrast to that pertaining to NT cloning in domestic animal species, since the MII oocytes of the latter lack cytoplasmic asters. Recent studies of microtubule configuration following somatic cell NT in cattle and pigs suggest a major contribution on the part of the donor cell centrosome (or centrosomal material, γ-tubulins) to the formation of the spindle that encloses the donor chromosomes, although newly appearing cytoplasmic asters are involved to a lesser extent [16, 17]. Interestingly, even when preactivated oocytes were used as recipients, these donor-derived centrosomes participated in the formation of spindles that were associated with the donor pronuclear-like structure and played a role in the positioning of this structure. These patterns are essentially

FIG. 5. Effect of Taxol on fragmentation induced in oocytes after delayed NT (Group C). A) Aster-like structures are formed in the cytoplasm 2 h after activation (arrows). B) Oocytes in the delayed NT group at 15 h after activation. These oocytes were treated with Taxol for 2 h before and after NT. Some of them retain normal appearance, but gradually undergo uneven cleavage (arrows) or mild fragmentation (arrowheads; compare with the severe fragmentation in C). Some of the oocytes that were treated with Taxol for 10 min after nuclear transfer cleaved and developed into blastocysts (inset). C) Oocytes in the delayed NT group without Taxol treatment. All of the oocytes have undergone complete fragmentation by 15 h after activation. Bar = 50 μm.

similar to that resulting from NT using blastomere nuclei [18]. Therefore, in domestic animal species the preactivated ooplasm that receives the donor nucleus develops through several cleavages, although very few of these ooplasts reach the blastocyst stage [3, 16]. Activated bovine oocytes that are enucleated at the telophase II stage have also proven to be suitable for NT [19], which indicates a certain amount of flexibility in the timing of NT and oocyte activation in the cloning of domestic species. In contrast, murine nuclear-transferred embryos from preactivated oocytes are never cleaved, and all of them undergo severe fragmentation during the first cell cycle [4, 5]. To date, only one cloned pup has been born from embryonic stem cells using preactivated oocytes that were chemically enucleated by demecolcine [20]. It would be interesting to know whether cytoplasmic asters persisted in these experiments, since as many as 36% of the reconstructed oocytes were cleaved [20]. An interval of 1 h between oocyte activation and NT is sufficient for fragmentation, as shown in this and previous studies [5]. Thus, murine somatic cell NT appears to be relatively inflexible in terms of the timing of oocyte activation and NT, although the reason for this is unclear.

The cytoskeletal dynamics observed during NT in this study indicate that the inability of murine preactivated oocytes to behave as appropriate recipients may be because of the lack of asters (or microtubule-nucleating activity) in the ooplasm at the time of NT. The cytoplasmic asters disappeared rapidly (within 2 h) after oocyte activation in all of the experimental groups, except for Group B, in which some asters remained for reasons unknown. Aster disappearance occurred irrespective of the presence or absence of the MII spindle (i.e., the oocytes in all the experimental groups, including the parthenogenetic group, had exactly the same pattern of aster disappearance). This phenomenon has also been noted with normally fertilized oocytes that were activated by spermatozoa [21, 22]. The disappearance of cytoplasmic asters from activated murine oocytes may reflect the loss of microtubule-nucleating activity. In the fertilized oocytes at S phase, a few γ-tubulin spots remained in the vicinity of the pronuclei, although well-developed cytoplasmic asters were not discernible.

The patterns of distribution of the fine microtubule networks in the cytoplasm, from which asters disappeared following activation, differed significantly among the experimental groups. The networks in the oocytes of the standard NT group (delayed activation) were distributed uniformly throughout the cytoplasm, whereas those in the delayed NT group showed irregular, patchy, or band distributions. The latter situation was also observed for enucleated oocytes that were activated without NT (Group E). In addition to these abnormal distributions of microtubules, we detected phalloidin-reactive actin filaments, which normally show a distinctive intense cortical band. It is known that contractile ring formation by actin filaments promotes cell division [23]. It seems unlikely that apoptosis is involved in this cascade, since there was no morphological evidence for apoptotic changes, such as nuclear splitting and chromatin aggregation, in the nuclei (data not shown). Therefore, the abnormal recruitment of actin filaments in delayed NT oocytes may lead directly to cytoplasmic fragmentation. However, the reason why abnormal distributions of microtubules and actin filaments occur in delayed NT oocytes remains unclear. To address this question, we treated delayed-NT oocytes with Taxol. This drug induces the formation of aster-like structures in activated oocytes. Therefore, the donor nucleus was introduced into oocyte cytoplasm that contained asters, as in standard NT. Interestingly, severe cytoplasmic fragmentation, which is inevitable in delayed NT oocytes, was not found in oocytes that were treated with Taxol for 3–4 h. However, Taxol induced abnormal cleavage or mild fragmentation (two to eight fragments) of oocytes, and we could not assess the developmental ability of the delayed-NT oocytes that were rescued by Taxol treatment. Therefore, in the second protocol, we treated the oocytes with Taxol for only 10 min to minimize the cytotoxicity of Taxol. As expected, fragmentation occurred in some oocytes owing to delayed NT, whereas the remaining oocytes escaped both fragmentation and Taxol toxicity and developed further. These findings clearly indicate that the presence of asters, or related microtubule nucleation activity, in the recipient ooplasm at the time of NT is crucial for the establishment of the normal nuclear-cytoskeletal configuration in nuclear-transferred oocytes. Thus, the use of MII oocytes is essential for successful mouse somatic cell cloning by NT, at least with regard to cytoskeletal dynamics.

Previously, it was reported that in the case of murine nuclear-transferred oocytes, normal chromatin reprogramming events, which include the silencing of donor nucleus transcription, the accumulation of TATA box-binding proteins, and increased DNase I sensitivity, occur only when the donor nucleus is introduced into MII-arrested recipient oocytes [6]. Chromatin reprogramming leads to zygotic gene activation at the appropriate time point after oocyte activation, and thereafter to normal embryo development. Taken together, our results and those of previous studies suggest that the use of MII oocytes as recipients in mouse cloning experiments is critical, not only for chromatin reprogramming but also for normal cytoskeletal organization in the reconstructed oocytes. This strict requirement is unique to murine somatic cell cloning.

ACKNOWLEDGMENTS

We thank Dr. Yukihiro Terada, Tohoku University, for his continued invaluable suggestions.

REFERENCES

1. Baguisi A, Behboodi E, Melican D, Pollock JS, Destrempes MM, Cammuso C, Williams JL, Nims SD, Porter CA, Midura P, Palacios MJ, Ayres SL, Denniston RS, Hayes ML, Ziomek CA, Meade HM, Godke RA, Gavin WG, Overstrom EW, Echelard Y. Production of goats by somatic nuclear transfer. Nat Biotech 1999; 17:456–461.
2. Campbell KHS, McWhir J, Ritchie WA, Wilmut I. Sheep cloned by nuclear transfer from a cultured cell line. Nature 1996; 380:64–66.
3. Tani T, Kato Y, Tsunoda Y. Direct exposure of chromosomes to non-activated ovum cytoplasm is effective for bovine somatic cell nucleus reprogramming. Biol Reprod 2001; 64:324–330.
4. Wakayama T, Perry ACF. Cloning of mice. In: Cibelli JB, Lanza R, Campbell K, West MD (eds.), Principles of Cloning. San Diego: Academic Press; 2002:301–341.
5. Wakayama T, Yanagimachi R. Effect of cytokinesis inhibitors, DMSO and the timing of oocyte activation on mouse cloning using cumulus cell nuclei. Reproduction 2001; 122:49–60.
6. Kim JM, Ogura A, Nagata M, Aoki F. Analysis of the mechanism for chromatin remodeling in embryos reconstructed by somatic nuclear transfer. Biol Reprod 2002; 67:760–766.
7. Schultz RM. Regulation of zygotic gene activation in the mouse. Bioessays 1993; 15:531–538.
8. Schatten H, Schatten G, Mazia D, Balczon R, Simerly C. Behavior of centrosomes during fertilization and cell division in mouse oocytes and sea urchin eggs. Proc Natl Acad Sci U S A 1986; 83:105–109.
9. Navara CS, Wu G-J, Simerly C, Schatten G. Mammalian model systems for exploring cytoskeletal dynamics during fertilization. Curr Topics Dev Biol 1995; 31:321–342.

10. Lawitts JA, Biggers JD. Culture of preimplantation embryos. Methods Enzymol 1993; 225:153–164.
11. Wakayama T, Perry ACF, Zuccotti M, Johnson KR, Yanagimachi R. Full-term development of mice from enucleated oocytes injected with cumulus cell nuclei. Nature 1998; 394:369–374.
12. Inoue K, Ogonuki N, Mochida K, Yamamoto Y, Takano K, Kohda T, Ishino F, Ogura A. Effects of donor cell type and genotype on the efficiency of mouse somatic cell cloning. Biol Reprod 2003; 69:1394–1400.
13. Chesne P, Adenot PG, Viglietta C, Baratte M, Boulanger L, Renard JP. Cloned rabbits produced by nuclear transfer from adult somatic cells. Nat Biotechnol 2002; 20:366–369.
14. Simerly C, Dominko T, Navara C, Payne C, Capuano S, Gosman G, Chong KY, Takahashi D, Chace C, Compton D, Hewitson L, Schatten G. Molecular correlates of primate nuclear transfer failures. Science 2003; 300:297.
15. Yin XJ, Kato Y, Tsunoda Y. Effect of enucleation procedures and maturation conditions on the development of nuclear-transferred rabbit oocytes receiving male fibroblast cells. Reproduction 2002; 124:41–47.
16. Shin M, Park S, Shim H, Kim N. Nuclear and microtubule reorganization in nuclear-transferred bovine embryos. Mol Reprod Dev 2002; 62:74–82.
17. Yin XJ, Cho SK, Park MR, Im YJ, Park JJ, Bhak JS, Kwon DN, Jun SH, Kim NH, Kim JH. Nuclear remodeling and the developmental potential of nuclear transferred porcine oocytes under delayed-activated conditions. Zygote 2003; 11:167–174.
18. Navara CS, First NL, Schatten G. Microtubule organization in the cow during fertilization, polyspermy, parthenogenesis, and nuclear transfer: the role of the sperm aster. Dev Biol 1994; 162:29–40.
19. Bordignon V, Smith LC. Telophase enucleation: an improved method to prepare recipient cytoplasts for use in bovine nuclear transfer. Mol Reprod Dev 1998; 49:29–36.
20. Gasparrini B, Gao S, Ainslie A, Fletcher J, McGarry M, Ritchie WA, Springbett AJ, Overstrom EW, Wilmut I, De Sousa PA. Cloned mice derived from embryonic stem cell karyoplasts and activated cytoplasts prepared by induced enucleation. Biol Reprod 2003; 68:1259–1266.
21. Maro B, Howlett SK, Webb M. Non-spindle microtubule organizing centers in metaphase II–arrested mouse oocytes. J Cell Biol 1985; 101:1665–1672.
22. Palacios MJ, Joshi HC, Simerly C, Schatten G. Gamma-tubulin reorganization during mouse fertilization and early development. J Cell Sci 1993; 104:383–389.
23. Cao L, Wang Y. Mechanism of the formation of contractile ring in dividing cultured animal cells. I. Recruitment of preexisting actin filaments into the cleavage furrow. J Cell Biol 1990; 110:1089–1095.

genesis 41:81–86 (2005)

LETTER

Birth of Mice Produced by Germ Cell Nuclear Transfer

Hiromi Miki,[1,2] Kimiko Inoue,[1] Takashi Kohda,[3] Arata Honda,[1] Narumi Ogonuki,[1] Misako Yuzuriha,[1] Nathan Mise,[1] Yasuhisa Matsui,[4] Tadashi Baba,[2] Kuniya Abe,[1] Fumitoshi Ishino,[3] and Atsuo Ogura[1]*

[1]RIKEN Bioresource Center, Tsukuba, Ibaraki, Japan
[2]Institute of Applied Biochemistry, University of Tsukuba, Tsukuba, Ibaraki, Japan
[3]Medical Research Institute, Tokyo Medical and Dental University, Chiyoda-ku, Tokyo, Japan
[4]Osaka Medical Center for Maternal and Child Health, Izumi, Osaka, Japan

Received 6 October 2004; Accepted 4 December 2004

Summary: That mammals can be cloned by nuclear transfer indicates that it is possible to reprogram the somatic cell genome to support full development. However, the developmental plasticity of germ cells is difficult to assess because genomic imprinting, which is essential for normal fetal development, is being reset at this stage. The anomalous influence of imprinting is corroborated by the poor development of mouse clones produced from primordial germ cells (PGCs) during imprinting erasure at embryonic day 11.5 or later. However, this can also be interpreted to mean that, unlike somatic cells, the genome of differentiated germ cells cannot be fully reprogrammed. We used younger PGCs (day 10.5) and eventually obtained four full-term fetuses. DNA methylation analyses showed that only embryos exhibiting normal imprinting developed to term. Thus, germ cell differentiation is not an insurmountable barrier to cloning, and imprinting status is more important than the origin of the nucleus donor cell per se as a determinant of developmental plasticity following nuclear transfer. genesis 41:81–86, 2005. © 2005 Wiley-Liss, Inc.

Key words: nuclear transfer; cloning; mouse; primordial germ cell; genomic imprinting

Since the birth of the sheep Dolly, the first eutherian mammal cloned from an adult cell, successful cloning using somatic cell nuclear transfer has been reported for the mouse, bovine, goat, pig, cat, rabbit, mule, horse, and rat (for review, see Tamada and Kikyo, 2004). Although the efficiency of cloning is low, it appears that at least some somatic cell genomes can acquire totipotency following transfer into enucleated oocytes. Somatic cell cloning is now being applied extensively to the production of clones of individuals, and to the generation of animals with genetic modifications for agricultural and pharmaceutical purposes. However, little is known about the developmental plasticity of the genome of the germ cell lineage. Only midgestation fetuses have been obtained from mouse primordial germ cells (PGCs), leading some to invoke "hemipotency" of the genome in the germ cell lineage (Kato *et al.*, 1999; Lee *et al.*, 2002; Yamazaki *et al.*, 2003). This limited efficiency of development of embryos cloned from PGCs may be attributed to the low plasticity of the germ cell genome attained during germ cell differentiation, or to erasure of the genomic imprinting "memory," known to occur in PGCs at embryo gestational day 11.5 in the mouse (Lee *et al.*, 2002).

Genomic imprinting in eutherian mammals is an epigenetic mechanism that ensures parent-allele-specific expression in some genes (imprinted genes) and plays essential roles in development and adult behavior (Reik and Walter, 2001; Li *et al.*, 1999). Imprinting "memories" are erased during early germ cell development and then reestablished in a parent-specific manner, depending on the sex of the individual. We previously examined the expression pattern of imprinted genes in fetuses cloned from fetal PGCs at embryo gestational days 11.5–13.5 (assuming the morning of the postcopulatory plug as day 0.5), and found that loss of their monoallelic expression proceeded stepwise from day 11.5 and was completed by day 12.5 (Lee *et al.*, 2002). Fetuses cloned from PGCs at days 12.5–13.5 arrested their development around day 8.5 in recipient foster mothers, as has been reported for PGCs at days 14.5–16.5 (Kato *et al.*, 1999). Those from nuclei of PGCs at day 11.5 developed furthest (to day 11.5), although they exhibited marked variation in their developmental potential, presumably reflecting the dynamic process of imprinting erasure in donor nuclei (Lee *et al.*, 2002). To extend this work, we created clones using PGCs from embryos at days 10.5 and 11.5 and examined whether such differentiated germ cell genomes could be fully reprogrammed by nuclear transfer. To ensure the accurate identification of PGCs, we used transgenic mice expressing green fluorescent protein (GFP) driven by the PGC-restricted *Oct-4* promoter (Yeom *et al.*,

Contact grant sponsors: MEXT (Japan), MHLW (Japan), CREST (Japan), Human Science Foundation (Japan).

*Correspondence to: Atsuo Ogura, D.V.M., Ph.D., RIKEN Bioresource Center, 3-1-1, Koyadai, Tsukuba, Ibaraki 305-0074, Japan.
E-mail: ogura@rtc.riken.go.jp

Published online 14 February 2005 in Wiley InterScience (www.interscience.wiley.com).
DOI: 10.1002/gene.20100

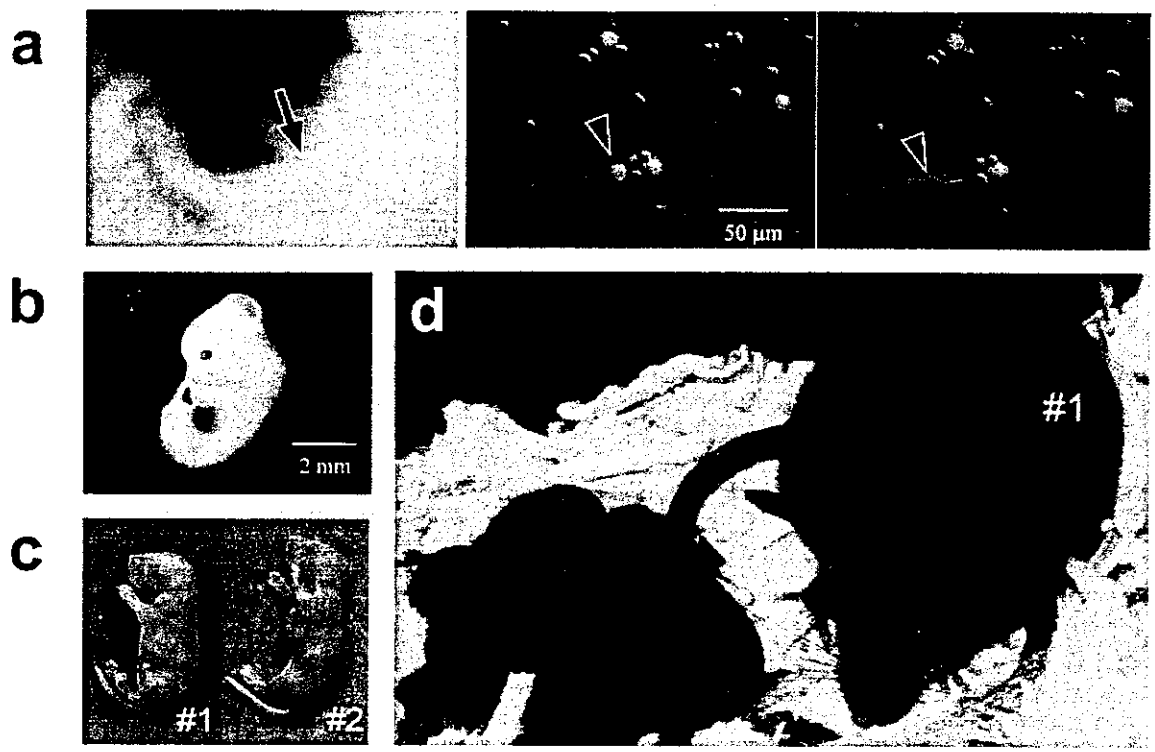

FIG. 1. Nuclear transfer with PGCs. **a:** PGCs reaching the genital ridges (arrow) at day 10.5 (left), and cells retrieved from the genital ridge at gestational day 10.5 (middle and right). PGCs were identified by their fluorescent markers and selected for nuclear transfer into enucleated oocytes (arrowheads). **b:** A gestational day 12.5 fetus cloned from a day 11.5 PGC. It was alive and appeared normal. As far as we examined, day 12.5 was the most advanced stage to which day 11.5 PGC clones could develop normally. **c:** Live female pups (#1 and #2) produced from day 10.5 PGCs by nuclear transfer. **d:** Both pups grew into normal adults and gave birth to offspring with normal litter sizes.

1996; Yoshimizu *et al.*, 1999) (Fig. 1a). We confirmed that all the GFP-expressing cells were positive for PGC7/Stella and alkaline phosphatase (data not shown), both of which are markers for mouse PGCs (Yoshimizu *et al.*, 1999; Saitou *et al.*, 2002; Sato *et al.*, 2002).

Approximately 60–80% of enucleated oocytes survived injection with PGC nuclei. When embryos were reconstructed with PGC nuclei from day 11.5 embryos (presumably in the G1 stage of the cell cycle), more than half of them cleaved within 24 h, and of these 63% reached the four-cell stage within the next 24 h (Table 1). These rates of development in vitro are similar to those reported previously (Lee *et al.*, 2002). Approximately 50% of the cloned embryos implanted following transfer into the oviducts of pseudopregnant females (Table 1). Live fetuses were retrieved at days 9.5, 10.5, 11.5, and 12.5, but not at days 13.5, 14.5, or 15.5 (Table 2). The three fetuses retrieved at days 11.5 and 12.5 appeared normal and had beating hearts (Fig. 1b). Thus, we concluded that day 12.5 was the most advanced stage of normal development that could be attained by embryos cloned from day 11.5 PGCs.

Based on these results, we evaluated the developmental potential of PGC nuclei from day 10.5 embryos. Cloned embryos reconstructed from these nuclei developed in vitro at a similar efficiency as those cloned from day 11.5 PGCs (Table 1). We reasoned that the relatively low cleavage rates of these PGC clones compared with those from cumulus cell or immature Sertoli cell nuclei (Ogura *et al.*, 2000a) could be attributable to rapid proliferation of the donor PGCs, which may cause cell cycle asynchrony between the recipient oocyte and the PGC nucleus. Embryos cloned from embryonic stem (ES) cells, which are also rapidly dividing cells, have shown a similar developmental pattern (Wakayama *et al.*, 1999). To test this possibility, we synchronized day 10.5 PGCs at metaphase by treatment with nocodazole and used the resulting cells as nuclear transfer donors. We found that the cleavage rate was indeed significantly improved ($P < 0.005$, Table 1). This strongly suggests that asynchrony of the cell cycle, not poor developmental plasticity of the PGCs, was the major cause of the one-cell arrest of these embryos cloned from PGCs. When 563 embryos reconstructed from day 10.5 PGCs were transferred into recipient females, 15 (2.7%) generated retrievable embryonic products at term (day 19.5). Of these, four contained fetuses (two alive and two stillborn), with the remaining 11 containing only a well-developed placenta with no associated fetus. The live-born PGC clones were both females that developed into normal adults of proven fertility (Fig. 1d).

Table 1
Development of Embryos Derived From Enucleated Oocytes Injected With Primordial Germ Cell (PGC) Nuclei

Day of PGC	Cell cycle	Method of nuclear transfer	No. cultured*	Cleaved (%)	4-cell (% of cleaved)	Transferred	Implanted (%)	Retrievable conceptuses at term (%)	Offspring (%)
11.5	Presumptive G1	Injection	1,512	831 (55.0)	543 (65.3)	521	256 (49.1)	–	–
10.5	Presumptive G1	Injection	2,018	1,011 (50.1)[a]	611 (60.4)	441	252 (57.1)	13 (2.9)	4 (0.9)
10.5	M	Fusion	269	189 (70.3)[b]	133 (70.4)	122	60 (49.2)	2 (1.6)	0 (0.0)
				(Day 10.5 PGC total)		962	508 (52.8)	15 (1.6)	4 (0.4)
Immature Sertoli cell	Presumptive G1	Injection	503	335 (66.6)	311 (92.8)	288	160 (55.6)	37 (12.8)	28 (9.7)

*Oocytes successfully injected (G1) or fused (M).
[a,b] $P < 0.005$ (one-way ANOVA).

Table 2
Number of Live Fetuses Retrieved Following Transfer of Embryos From Day 11.5 PGCs

Day of gestation	No. live fetuses/ those implanted
9.5	6/173
10.5	6/62
11.5	2/30
12.5	1/47
13.5	0/14
14.5	0/82
15.5	0/113

We analyzed the DNA methylation status of differentially methylated regions of imprinted genes in day 11.5 PGC clones surviving to midgestation and the day 10.5 PGC clones that reached term. All placental and tail-tip tissues examined contained both a methylated and an unmethylated allele for *Peg5/Nnat, Peg3,* and *H19*, each indistinguishable from its respective normal methylation imprint (Fig. 2). The timing of methylation erasure relative to other imprinted genes is early for *Peg5/Nnat* and *Peg3*, and is intermediate for *H19* (Lee *et al.*, 2002). Moreover, the imprinting status of clones may reflect that of their respective nucleus donors (Inoue *et al.*, 2002). This suggests that normal development was restricted to those PGC donor nuclei that retained parental imprinted memory for most, if not all, imprinted genes. The difference in developmental ability of clones derived from PGC nuclei at days 10.5 and 11.5 thus probably reflects a subpopulation of PGCs that had not initiated erasure of their imprinting memory. This assumption is consistent with results from analysis of the DNA methylation status of imprinted genes in donor PGCs at days 10.5–12.5. These cells are heterologous populations in terms of their DNA methylation status, as the former group has more nuclei exhibiting monoallelic methylation marks that have not yet been erased (Lee *et al.*, 2002). However, a recent study showing the full-term development of parthenogenetically reconstructed embryos indicates that the control of imprinted gene expression levels is more complex than we had thought (Kono *et al.*, 2004). The expression levels of certain genes (*H19* and *Igf2*, and probably *Gtl2* and *Dlk1*) apparently affected the expression profiles of a broad range of other imprinted genes, and thus determined the developmental potential of embryos. It will be interesting to see whether the same is true for the development of clones from PGC. A wide-range analysis using cloned fetuses from midgestation PGCs would settle this question.

All term placentas of conceptuses cloned from day 10.5 PGCs, including the placenta-only ones, showed hypertrophic development, characteristic of somatic cell clones in the mouse (Fig. 3) (Wakayama and Yanagimachi, 1999a). This placental hypertrophy, together with the frequent postimplantation loss of such embryos (Wakayama and Yanagimachi, 1999b), indicates that the genomes of day 10.5 PGCs still retain a somatic cell genome type in

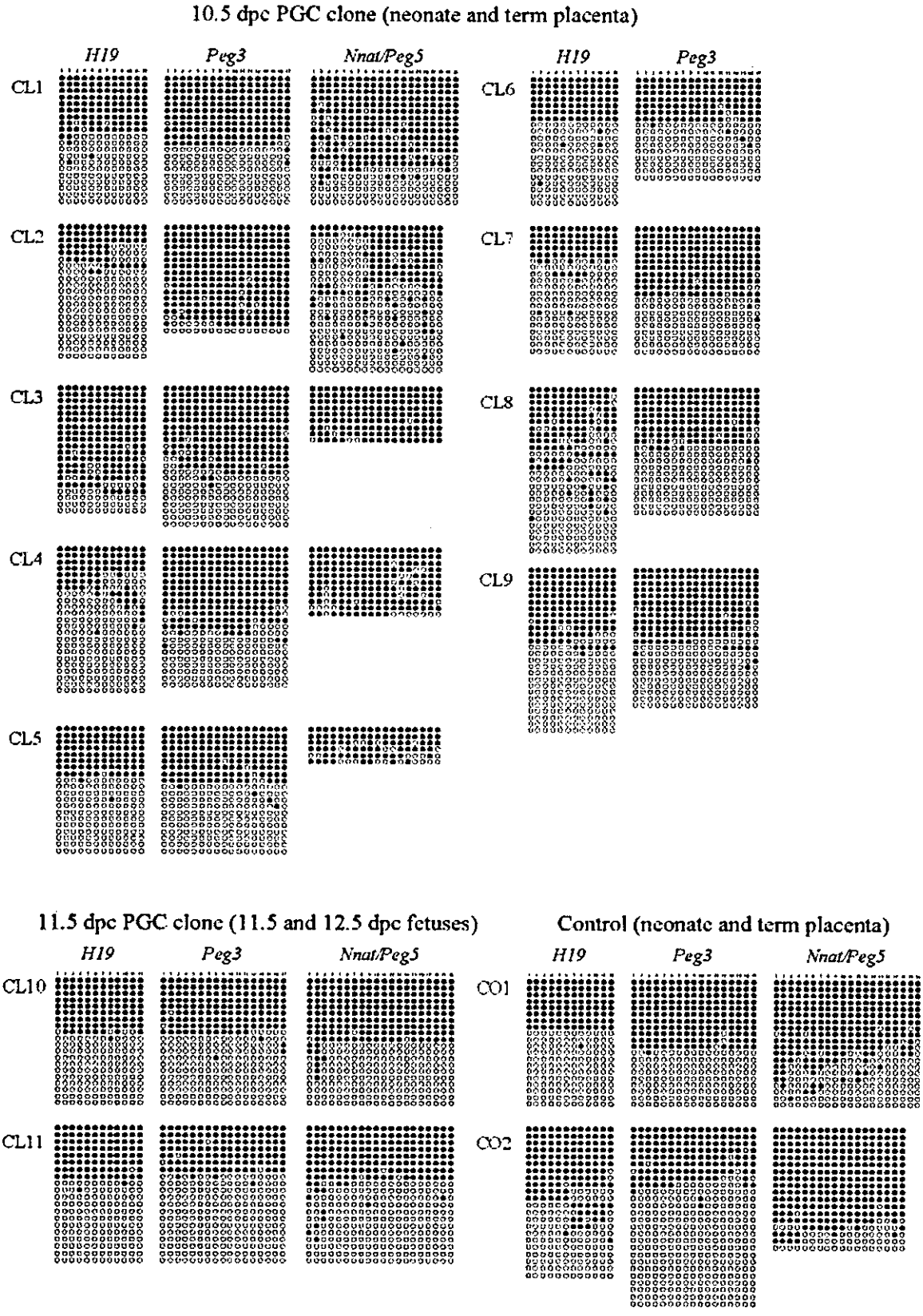
10.5 dpc PGC clone (neonate and term placenta)
H19
Peg3
Nnat/Peg5
CL1
CL2
CL3
CL4
CL5
H19
Peg3
CL6
CL7
CL8
CL9
11.5 dpc PGC clone (11.5 and 12.5 dpc fetuses)
H19
Peg3
Nnat/Peg5
CL10
CL11
Control (neonate and term placenta)
H19
Peg3
Nnat/Peg5
CO1
CO2

FIG. 2

terms of their reprogrammability in the egg cytoplasm. It is reasonable to assume that the female (oocyte) and male (sperm) germ cell genomes undergo some epigenetic modifications during their early development, so that they can be correctly reprogrammed at fertilization to participate in the formation of a totipotent zygotic genome (Fulka *et al.*, 2004). Somatic cell genomes presumably bypass this process and therefore are erroneously reprogrammed when transferred into the egg cytoplasm (Dean *et al.*, 2001). Our results indicate that this (unknown) epigenetic modification process—if present—must exist at day 11.5 or later in the mouse.

Differentiation of the germ cells equips them uniquely to transmit their genome to the next generation. We have shown here that PGCs recovered as late as gestational day 10.5 are able to support full development following nuclear transfer. This suggests that the germ cell genome can be fully reprogrammed even after the PGCs have undergone distinctive differentiation (Saitou *et al.*, 2002; McLaren, 2003) and have reached the genital ridge (typically around day 10.5 in the mouse). These findings support the hypothesis that, in general, imprinting status is more important than the origin of the nucleus donor cell per se as a determinant of definitive developmental plasticity following nuclear transfer.

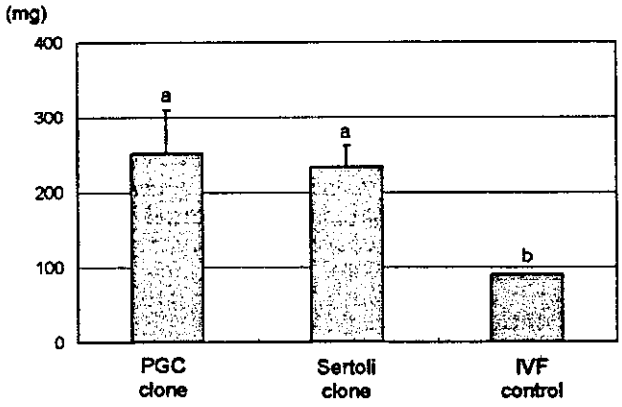

FIG. 3. Placental weights of clones and in vitro fertilization (IVF) controls at term. The mean weights of placentas cloned from day 10.5 PGCs (n = 15) and from immature Sertoli cells (n = 11) were significantly larger than those of genotype-matched IVF controls (n = 14). There was no significant difference in mean placental weight between PGC and Sertoli cell clones. $^{a,b}P < 0.05$ (by Scheffe's F-test). Error bar = SEM.

MATERIALS AND METHODS

Preparation of Donor Cells

For preparation of donor PGCs, B6D2F1 females were mated with *Oct-4*/GFP transgenic males (GOF-18/delta PE/GFP, 129/Sv-*ter* background), and sacrificed at days 10.5 or 11.5 of embryonic development. The PGC-specificity of GFP fluorescence was endowed by the *Oct-4* fragment transgene in the genome of strain GOF-18/delta PE (Yeom *et al.*, 1996; Yoshimizu *et al.*, 1999). Genital ridges were removed from fetuses and treated with 0.1 mg collagenase (Sigma, St. Louis, MO) in Complete Blastocyst Medium (CBM) (Irvine Scientific, Santa Ana, CA) at 37°C for 40 min to suspend single cells. The media used for culturing PGCs were kept serum-free throughout to avoid alteration of the genomic imprinting status of PGCs (Khosla *et al.*, 2001).

Nuclear Transfer

Nuclear transfer was carried out as described (Wakayama *et al.*, 1998; Ogura *et al.*, 2000b; Inoue *et al.*, 2003). The oocytes were collected from 8-week-old B6D2F1 females superovulated by injection with PMSG (7.5 IU) and hCG (7.5 IU) at 48-h intervals. At 15 h after the hCG injection, cumulus-oocyte complexes were collected from the oviducts and the cumulus cells were allowed to disperse in KSOM medium (Lawitts *et al.*, 1993) that contained 0.1% bovine testicular hyaluronidase (Sigma). The oocytes were enucleated in Hepes-buffered KSOM medium containing 7.5 μg/mL cytochalasin B (Calbiochem, San Diego, CA). The nuclei from PGCs were transferred into enucleated oocytes using intracytoplasmic injection with piezo-driven micromanipulators (Primetech, Ibaraki, Japan: Wakayama *et al.*, 1998; Inoue *et al.*, 2003), or by electrofusion (Ogura *et al.*, 2000b). In initial experiments, we selected relatively small PGCs (~15 μm in diameter) for nuclear transfer, in attempts to select relatively homogeneous populations that would be compatible with recipient oocytes. In later experiments, PGCs were arrested at metaphase by exposure to 0.4 μg nocodazole (Sigma) in CBM for 4 h and subsequently used for nuclear transfer by electrofusion. Unlike experiments on nuclear transfer using nontreated PGCs, following the transfer of presumptively post-S-phase nocodazole-treated PGCs the polar body containing its donor sister chromosomes was extruded to restore diploidy. Oocytes successfully injected or fused with donor PGCs were cultured in

FIG. 2. Bisulfite genomic sequence analysis of PGC clones. Fetuses, term placentas, and neonates were analyzed for *H19, Peg3,* and *Nnat/Peg5* in day 10.5 PGC clones, day 11.5 PGC clones, and controls. Open circles represent unmethylated CpG sequences, and filled circles indicate methylated CpGs. All of the placental and tail-tip tissues examined contained methylated and unmethylated alleles for *Peg5/Nnat, Peg3,* and *H19* that were indistinguishable from their respective normal methylation imprints, except for hypermethylated *Peg3* alleles in the second clone. For some term placentas, the *Nnat/Peg5* sequences were not analyzed because this gene showed tissue-specific hypermethylation in placentas, including the control (CO2). CL1, first live day 10.5 PGC clone neonate (tail-tip); CL2, second live day 10.5 PGC clone neonate (tail-tip); CL3, stillborn PGC clone (placenta); CL4-9, placenta-only conceptus at term; CL10, a gestational day 11.5 fetus cloned from a day 11.5 PGC; CL11, a gestational day 12.5 fetus cloned from a day 11.5 PGC; CO1, control IVF neonate (tail-tip); CO2, control IVF term placenta.

KSOM medium for 48 h and four-cell embryos were transferred into the oviducts of day 0.5 ICR strain pseudopregnant females, which had been mated with vasectomized males. The recipient females were examined for the presence of conceptuses at midgestation or term by cesarean section. Retrieved term fetuses were nursed by lactating ICR females. Control embryos were produced by nuclear transfer using immature Sertoli cells (Ogura *et al.*, 2000a) or by conventional in vitro fertilization (IVF) (Toyoda *et al.*, 1989).

DNA Methylation Analysis

Genomic DNA was prepared from fetuses, placentas, and tail-tip tissues of PGC clones and genotype-matched controls, using ISOGEN (Nippon Gene, Japan). Purified DNA was treated with a sodium bisulfite solution as described previously (Raizis *et al.*, 1995). The *H19* promoter region, the 5′ upstream region of *Peg3*, and the 5′ upstream region of *Peg5* were amplified using *ExTaq* DNA polymerase (TaKaRa, Japan) for 30 cycles under the following conditions: 96°C for 15 s, 60°C for 30 s, and 72°C for 30 s. The PCR primers used were as follows: H19 bi F: 5′-GGA ATA TTT GTG TTT TTG GAG GG-3′; H19 bi R: 5′-TTA AAC CCC AAC CTC TAC TTT TAT AAC-3′; Peg3-CT-IF: 5′-TTT TGT AGA GGA TTT TGA TAA GGA GG-3′; Peg3-CT-IR2: 5′-CCC CAA ACA CCA TCT AAA CTC TAC-3′; Peg5 bi F: 5′-GAG GAT ATA AGT TTT ATT TTG AAA TTA GAA G-3′; Peg5 bi R: 5′-TAC CTT AAA TAC CCT CTT ACC ACC TAA A-3′.

Amplified fragments were cloned into the plasmid vector pGEM-T Easy (Promega, Madison, WI) and sequenced using BigDye Terminator Cycle Sequencing Kit (v. 3.1) using an ABI PRISM 3100 Genetic Analyzer (Applied Biosystems, Foster City, CA).

Statistical Analysis

The proportions of embryos that reached two cells, four cells, or term were transformed using arcsine transformation and analyzed by repeated-measure one-way ANOVA. The weights of placentas from clones and controls were analyzed by repeated-measure one-way ANOVA, followed by a multiple comparison test (Scheffe's F-test). $P < 0.05$ was assumed statistically significant.

ACKNOWLEDGMENTS

We thank Dr. Toru Nakano for kindly providing the antibody for PGC7 and Mr. Satoru Kobayakawa for staining the PGCs with this antibody.

LITERATURE CITED

Dean W, Santos F, Stojkovic M, Zakhartchenko V, Walter J, Wolf E, Reik W. 2001. Conservation of methylation reprogramming in mammalian development: Aberrant reprogramming in cloned embryos. Proc Natl Acad Sci U S A 98:13734-13738.

Fulka J Jr, Miyashita N, Nagai T, Ogura A. 2004. Do cloned mammals skip a reprogramming step? Nat Biotechnol 22:25-26.

Inoue K, Kohda T, Lee J, Ogonuki N, Mochida K, Noguchi Y, Tanemura K, Kaneko-Ishino T, Ishino F, Ogura A. 2002. Faithful expression of imprinted genes in cloned mice. Science 295:297.

Inoue K, Ogonuki N, Mochida K, Yamamoto Y, Takano K, Kohda T, Ishino F, Ogura A. 2003. Effects of donor cell type and genotype on the efficiency of mouse somatic cell cloning. Biol Reprod 69:1394-1400.

Kato Y, Rideout WM III, Hilton K, Barton SC, Tsunoda Y, Surani MA. 1999. Developmental potential of mouse primordial germ cells. Development 126:1823-1832.

Khosla S, Dean W, Brown D, Reik W, Feil R. 2001. Culture of preimplantation mouse embryos affects fetal development and the expression of imprinted genes. Biol Reprod 64:918-926.

Kono T, Obata Y, Wu Q, Niwa K, Ono Y, Yamamoto Y, Park ES, Seo JS, Ogawa H. 2004. Birth of parthenogenetic mice that can develop to adulthood. Nature 428:860-864.

Lawitts JA, Biggers JD. 1993. Culture of preimplantation embryos. Methods Enzymol 225:153-164.

Lee J, Inoue K, Ono R, Ogonuki N, Kohda K, Kaneko-Ishino T, Ogura A, Ishino F. 2002. Erasing genomic imprinting memory in mouse clone embryos produced from day 11.5 primordial germ cells. Development 129:1807-1817.

Li L, Keverne EB, Aparicio SA, Ishino F, Barton ,SC, Surani MA. 1999. Regulation of maternal behavior and offspring growth by paternally expressed *Peg3*. Science 284:330-333.

McLaren A. 2003. Primordial germ cells in the mouse. Dev Biol 262:1-15.

Ogura A, Inoue K, Ogonuki N, Noguchi A, Takano K, Nagano R, Suzuki O, Lee J, Ishino F, Matsuda J. 2000a. Production of male clone mice from fresh, cultured, and cryopreserved immature Sertoli cells. Biol Reprod 62:1579-1584.

Ogura A, Inoue K, Takano K, Wakayama T, Yanagimachi R. 2000b. Birth of mice after nuclear transfer by electrofusion using tail tip cells. Mol Reprod Dev 57:55-59.

Raizis AM, Schmitt F, Jost JP. 1995. A bisulfite method of 5-methylcytosine mapping that minimizes template degradation. Anal Biochem 226:161-166.

Reik W, Walter J. 2001. Genomic imprinting: parental influence on the genome. Nat Rev Genet 2:21-32.

Saitou M, Barton SC, Surani MA. 2002. A molecular programme for the specification of germ cell fate in mice. Nature 418:293-300.

Sato M, Kimura T, Kurokawa K, Fujita K, Abe K, Masuhara M, Yasunaga T, Ryo A, Yamamoto M, Nakano T. 2002. Identification of PGC7, a new gene expressed specifically in preimplantation embryos and germ cells. Mech Dev 113:91-94.

Tamada H, Kikyo N. 2004. Nuclear reprogramming in mammalian somatic cell nuclear cloning. Cytogenet Genome Res 105:285-291.

Toyoda Y, Azuma S, Takeda S. 1989. Effects of chelating agents on preimplantation development of mouse embryos fertilized in vitro. Prog Clin Biol Res 294:171-179.

Wakayama T, Yanagimachi R. 1999a. Cloning of male mice from adult tail-tip cells. Nat Genet 22:127-128.

Wakayama T, Yanagimachi R. 1999b. Cloning the laboratory mouse. Semin Cell Dev Biol 10:253-258.

Wakayama T, Perry ACF, Zuccotti M, Johnson KR, Yanagimachi R. 1998. Full-term development of mice from enucleated oocytes injected with cumulus cell nuclei. Nature 394:369-374.

Wakayama T, Mombaerts P, Rodriguez I, Perry ACF, Yanagimachi R. 1999. Mice cloned from embryonic stem cells. Proc Natl Acad Sci U S A 96:14984-14989.

Yamazaki Y, Mann MRW, Lee SS, Marh J, McCarrey JR, Yanagimachi R, Bartolomei MS. 2003. Reprogramming of primordial germ cells begins before migration into the genital ridge, making these cells inadequate donors for reproductive cloning. Proc Natl Acad Sci U S A 100:12207-12212.

Yeom YI, Fuhrmann G, Ovitt CE, Brehm A, Ohbo K, Gross M, Hubner K, Scholer HR. 1996. Germline regulatory element of Oct-4 specific for the totipotent cycle of embryonal cells. Development 122:881-894.

Yoshimizu T, Sugiyama N, DeFelice M, Yeom YI, Ohbo K, Masuko K, Obinata M, Abe K, Scholer HR, Matsui Y. 1999. Germline-specific expression of the Oct-4/green fluorescent protein (GFP) transgene in mice. Dev Growth Differ 41:675-684.

Cell, Vol. 119, 1001–1012, December 29, 2004, Copyright ©2004 by Cell Press

Generation of Pluripotent Stem Cells from Neonatal Mouse Testis

Mito Kanatsu-Shinohara,[1] Kimiko Inoue,[5] Jiyoung Lee,[6] Momoko Yoshimoto,[4] Narumi Ogonuki,[5] Hiromi Miki,[5] Shiro Baba,[4] Takeo Kato,[4] Yasuhiro Kazuki,[7] Shinya Toyokuni,[2] Megumi Toyoshima,[3] Ohtsura Niwa,[3] Mitsuo Oshimura,[7] Toshio Heike,[4] Tatsutoshi Nakahata,[4] Fumitoshi Ishino,[6] Atsuo Ogura,[5] and Takashi Shinohara[1,8,*]

[1]Horizontal Medical Research Organization
[2]Department of Pathology and Biology of Diseases
Graduate School of Medicine
[3]Radiation Biology Center
Kyoto University
Kyoto 606-8501
[4]Department of Pediatrics
Graduate School of Medicine
Kyoto University
Kyoto 606-8507
[5]The Institute of Physical and Chemical Research
RIKEN
Bioresource Center
Ibaraki 305-0074
[6]Medical Research Institute
Tokyo Medical and Dental University
Tokyo 101-0062
[7]Department of Molecular and Cell Genetics
School of Life Sciences
Faculty of Medicine
Tottori University, Yonago
Tottori 683-8503
Japan

Summary

Although germline cells can form multipotential embryonic stem (ES)/embryonic germ (EG) cells, these cells can be derived only from embryonic tissues, and such multipotent cells have not been available from neonatal gonads. Here we report the successful establishment of ES-like cells from neonatal mouse testis. These ES-like cells were phenotypically similar to ES/EG cells except in their genomic imprinting pattern. They differentiated into various types of somatic cells in vitro under conditions used to induce the differentiation of ES cells and produced teratomas after inoculation into mice. Furthermore, these ES-like cells formed germline chimeras when injected into blastocysts. Thus, the capacity to form multipotent cells persists in neonatal testis. The ability to derive multipotential stem cells from the neonatal testis has important implications for germ cell biology and opens the possibility of using these cells for biotechnology and medicine.

*Correspondence: takashi@mfour.med.kyoto-u.ac.jp
[8]Present address: Department of Molecular Genetics, Graduate School of Medicine, Kyoto University, Kyoto 606-8507, Japan.

Introduction

Germ cells are unique in that they have the capacity to contribute genes to offspring. Although germ cells are highly specialized cells for the generation of gametes, several lines of evidence suggest their multipotentiality. For example, teratomas are tumors containing many kinds of cells and tissues at various stages of maturation, which occur almost exclusively in the gonads (Stevens, 1984). Furthermore, primordial germ cells (PGCs) from embryos between 8.5 and 12.5 days postcoitum (dpc) give rise to pluripotent cells when cultured under appropriate conditions (Resnick et al., 1992; Matsui et al., 1992). These EG cells have differentiation properties similar to ES cells isolated from inner cell mass (Martin, 1981; Evans and Kaufman, 1981). While these observations suggest that the germline lineage retains the ability to generate pluripotent cells, it has not been possible to establish pluripotent cells from normal neonatal gonads (Labosky et al., 1994).

We recently reported the in vitro culture of mouse spermatogonial stem cells (Kanatsu-Shinohara et al., 2003a), the only type of stem cell in the body that transmits genetic information to offspring (Meistrich and van Beek, 1993; de Rooij and Russell, 2000). When neonatal testis cells were cultured in the presence of glial cell line-derived neurotrophic factor (GDNF), leukemia inhibitory factor (LIF), epidermal growth factor (EGF), and basic fibroblast growth factor (bFGF), the germ cells developed uniquely shaped colonies, and the stem cells proliferated logarithmically over a 5 month period. Upon transplantation into the seminiferous tubules of infertile mice, the cultured cells produced normal sperm and offspring, and neither somatic differentiation nor teratoma formation was observed, indicating that the cultured cells were fully committed to the germ cell lineage (Kanatsu-Shinohara et al., 2003a). This was in contrast to ES cells, which produced teratoma after being transferred into seminiferous tubules (Brinster and Avarbock, 1994). Based on these results, we named these cells germline stem (GS) cells to distinguish them from ES or EG cells. Thus, GS cells represent a third method of expanding germline cells, but they are clearly distinct from ES/EG cells in their differentiation capacity.

In this manuscript, we describe the derivation of pluripotent stem cells from the neonatal mouse testis. Neonatal testis cells were cultured in conditions similar to those used for GS cell culture. In addition to the GS cell colonies, colonies indistinguishable from ES cell colonies appeared. This second cell type could be expanded selectively under culture conditions used for ES cells. Although they produced teratomas when transplanted subcutaneously or into the seminiferous tubules of the testis, they participated in normal embryonic development following injection into blastocysts.

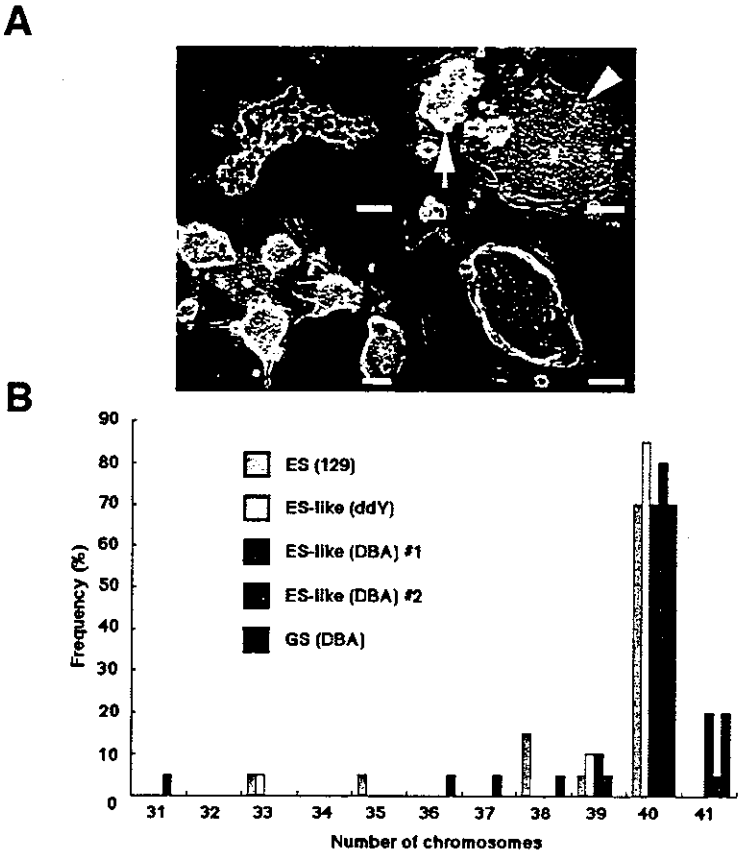

Figure 1. ES-Like Colonies from Neonatal Testis Cells

(A) Morphology of ES-like cells. (Top, left) A typical colony of GS cells. (Top, right) ES-like colony (arrow) and cultured epiblast-like colony (arrowhead), which appeared under GS cell culture conditions, at 40 days after the initiation of culture. (Bottom, left) Established culture of ES-like cells at 50 days. (Bottom, right) A typical colony of ES-like cells at 95 days.

(B) Distribution of metaphase spreads with different chromosome numbers. At least 20 cells were counted. Scale bar, 50 μm.

Results

Development of ES-Like Colonies from Neonatal Testis Cells in the Presence of Growth Factors

When neonatal ddY mouse testis cells were cultured in a primary medium containing GDNF, bFGF, EGF, and LIF, the majority of the colonies that formed had the typical appearance of GS cells, which are characterized by intercellular bridges and a morula-like structure (Figure 1A, top left) (Kanatsu-Shinohara et al., 2003a). However, we occasionally found colonies that were remarkably similar to ES cells or cultured epiblast cells (Figure 1A, top right) (Kanatsu and Nishikawa, 1996). These colonies were more tightly packed and generally appeared within 4–7 weeks after initiation of the culture (~four to seven passages). After these ES cell-like colonies appeared, they outgrew the GS cells and became the dominant population within 2–3 weeks. Although these ES-like colonies generally differentiated to lose their ES cell-like appearance after several passages under GS cell culture conditions, they retained ES-like appearance and could be selectively expanded when cultured in a secondary medium containing 15% fetal calf serum (FCS) and LIF (standard ES cell culture conditions).

After two to three passages, most colonies in the culture consisted of these ES-like colonies (Figure 1A, bottom left), which could be maintained with standard ES cell culture conditions. In contrast, GS cells could not be propagated under these conditions due to the absence of GDNF, an essential growth factor for the self-renewing division of spermatogonial stem cells (Meng et al., 2000). Cytogenetic analysis by quinacrine plus Hoechst 33258 staining showed that the ES-like cells had a normal karyotype (40, XY) in 70%–85% of metaphase spreads (Figure 1B). The morphology of the ES-like cells did not change as long as the cells were maintained in ES cell culture conditions, and they could be propagated in vitro for more than 5 months with 48 passages while maintaining an undifferentiated state (Figure 1A, bottom right). Established cultures were passed at a dilution of 1:3 to 1:6 every 3 days.

These results were reproducible; similar cells were obtained from mice with a different genotype (DBA/2), and ES-like cells were successfully established in four of 21 experiments (19%). The overall frequency of forming ES-like cells was 1 in 1.5×10^7 cells (equivalent to ~35 newborn testes). Significantly, neither GS nor ES-like cells appeared when newborn testis cells were cultured directly in ES culture conditions in at least 20 experiments. Likewise, neither GS nor ES-like cells appeared when neonatal testis cells were cultured in the presence of membrane bound Steel factor (mSCF), LIF, and bFGF (EG cell culture condition) in at least 15 experiments; the addition of GDNF was a prerequisite for the development of both GS and ES-like colonies. In addition, when CD9-selected adult spermatogonial stem cells from 3- to 8-week-old mice were cultured (Kanatsu-Shinohara et al., 2004), GS cells appeared in three of 15

experiments, but no ES-like cells appeared. We also did not observe GS or ES-like cell colonies when male genital ridges from 12.5 dpc embryos were cultured in GS cell medium in 12 experiments.

Development of ES-Like Colonies from GS Cells Derived from p53 Knockout Mice

To determine whether GS cells can convert to ES-like cells, we picked a total of 266 GS cell colonies by micromanipulation at 2 months after culture initiation. These GS cells were transferred to a 96-well plate and expanded for an additional 3 months, but none of them became ES-like cells. Although the result strongly suggested the distinct origin of ES-like cells, it was still possible that the conversion occured at lower frequency. To address this possibility, we used p53 knockout mice (Tsukada et al., 1993), which have a high frequency of testicular teratoma (Lam and Nadeau, 2003). We hypothesized that ES-like cells have a close relationship with teratoma-forming cells and asked whether established GS cells from this strain convert more easily to ES-like cells. GS cells were established from a newborn p53 knockout mouse in an ICR background. The growth speed and morphology of GS cells were indistinguishable from those of wild-type cells, and GDNF was similarly required to obtain GS cells.

Two months after culture, 30–40 GS cell colonies of undifferentiated morphology were picked by micromanipulation, transferred to a 96-well plate, and cultured in GS cell culture medium. Significantly, ES-like cells appeared in these GS cell-derived cultures in two separate experiments within 2 months, and the colonies were morphologically indistinguishable from ES-like colonies from wild-type cells. Interestingly, although ES-like cells never appeared from fully established wild-type GS cells after long-term culture, p53 knockout GS cells produced ES-like cells as long as 6 months after the initiation of culture.

Using p53 knockout mice, we also examined whether GS cells from mature testis can produce ES-like cells. Spermatogonial stem cells were collected from 3- to 8-week-old mice using anti-CD9 antibody and cultured in GS cell medium. GS cells developed in two of three experiments. GS cells of undifferentiated morphology were picked 4–7 days after culture initiation, and the colonies were expanded in vitro on mitomycin C-inactivated mouse embryonic fibroblast (MEF). In total, ES-like cells appeared in two of eight experiments within 4 weeks of culture.

Phenotypic Analysis of ES-Like Cells

To examine the phenotype of the ES-like cells, we established a population from a newborn transgenic mouse line C57BL6/Tg14(act-EGFP-OsbY01) that was bred into the DBA/2 background (designated Green). Since these Green mice express the enhanced green fluorescence protein (EGFP) gene ubiquitously, including in spermatogenic cells (Kanatsu-Shinohara et al., 2003a), cultured cells can be distinguished from feeder cells under excitation with UV light. The ES-like cells comprised a single phenotypic population by flow cytometric analysis of surface antigens (Figure 2A). They were strongly positive for SSEA-1 (ES cell marker) (Solter and Knowles, 1978), EE2 (spermatogonia marker) (Koshimizu et al., 1995), β1- and α6-integrin (GS cell marker) (Kanatsu-Shinohara et al., 2003a), CD9 (ES and GS cell marker) (Kanatsu-Shinohara et al., 2004), and EpCAM (ES and spermatogonia cell marker) (Anderson et al., 1999). The ES-like cells were weakly positive for Forssman antigen (ES cell marker) (Evans and Kaufman, 1981) and c-kit (differentiated spermatogonia marker) (Schrans-Stassen et al., 1999). In contrast, GS cells were completely negative for SSEA-1 and Forssman antigen, confirming that ES-like cells are phenotypically distinct from GS cells. GS cells from p53 knockout mice showed similar expression profile (data not shown). Although we found some expression of Forssman antigen in the neonatal testis cell population before culture, it was expressed by a non-germ cell population, and no SSEA-1-positive cells were found (Figures 2A and 2B). The ES-like cells were also strongly positive for alkaline phosphatase (ALP), which is characteristic of ES and EG cells (Resnick et al., 1992; Matsui et al., 1992) (Figure 2C).

Next, we used the reverse transcriptase-polymerase chain reaction (RT-PCR) to examine several molecules that are specifically expressed in embryonal carcinoma (EC) or ES cells. In addition to Oct-4, Rex-1, and Nanog, which are essential for maintaining undifferentiated ES cells (Pesce and Schöler, 2001; Goolsby et al., 2003; Mitsui et al., 2003; Chambers et al., 2003), the ES-like cells expressed Cripto, ERas, UTF1, Esg-1, and ZFP57 at similar levels to ES cells (Kimura et al., 2001; Takahashi et al., 2003; Okuda et al., 1998; Tanaka et al., 2002; Ahn et al., 2004). GS cells also expressed some of these molecules, but the expression was generally weaker. Significantly, we could not detect expression of Nanog in GS cells, suggesting that they have a different mechanism for self-renewal from that of ES cells (Figure 2D).

Analysis of Genomic Imprinting in ES-Like Cells

To analyze the imprinting pattern of ES-like cells, differentially methylated regions (DMRs) of three paternally imprinted regions (*H19*, *Meg3 IG*, and *Rasgrf1* regions) and two maternally imprinted regions (*Igf2r* and *Peg10* regions) were examined by bisulfite sequencing with two independent cells (Figure 3A). While the paternally imprinted regions were methylated to different degrees, the maternally imprinted regions were rarely methylated in ES-like cells. DMRs in ES cells were generally more methylated than those in ES-like cells, including maternally imprinted regions, and the DMRs of the *H19* region were methylated more extensively than the DMRs of other regions. In contrast, GS cells showed a complete androgenetic imprinting pattern: the complete methylation of both the *H19* and *Meg3 IG* DMRs and demethylation of the *Igf2r* DMR.

Next, we examined the imprint status of GS or ES-like cells from p53 knockout mice. Genomic DNA was isolated from the same cell population at four different time points during the conversion of GS cells into ES-like cells. In these experiments, the imprint status in the DMRs was determined by combined bisulfite restriction analysis (COBRA) (Xiong and Laird, 1997) (Figure 3B). As expected from the analysis of wild-type GS cells, GS

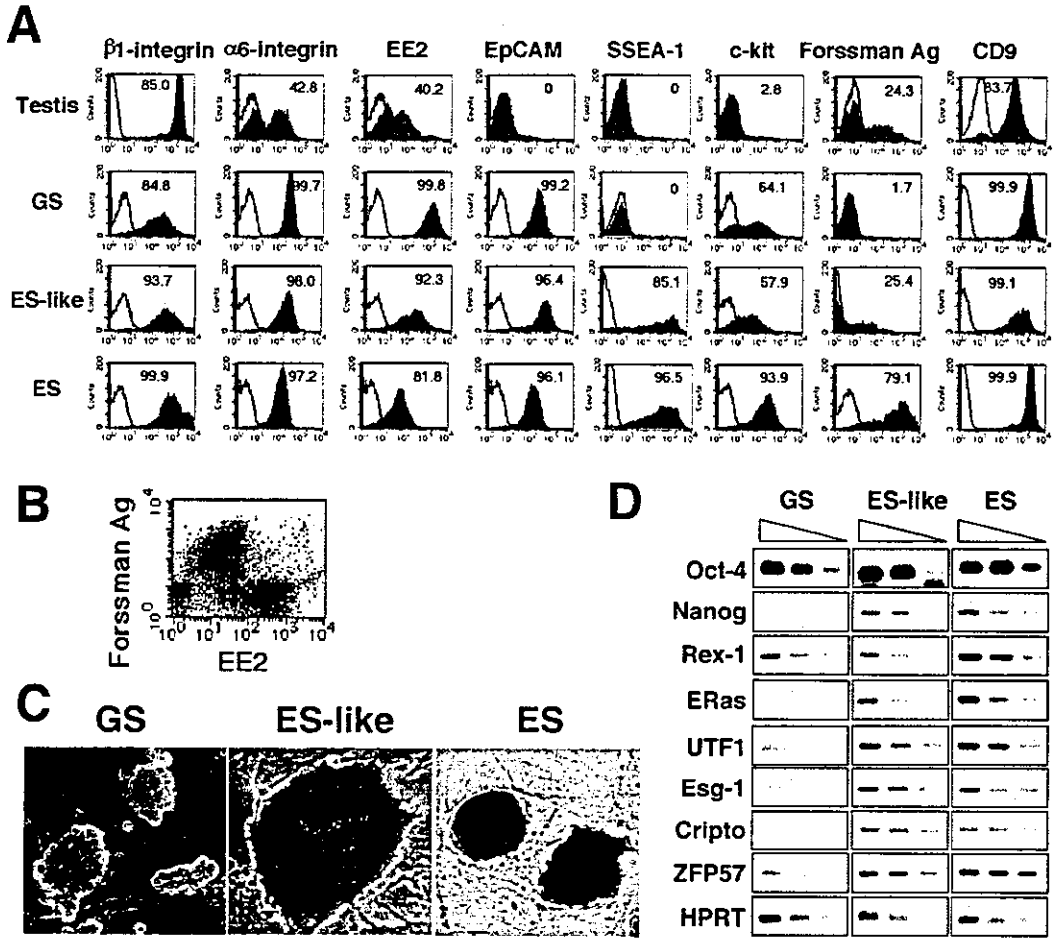

Figure 2. Phenotypic Characterization of ES-Like Cells

(A) Flow cytometric characterization of ES-like cells. Black line, control immunoglobulin; red line, specific antibody.

(B) Double immunostaining of neonatal testis cells by anti-EE2 and anti-Forssman antigen antibodies.

(C) ALP staining. GS cells (left) are weakly positive, whereas ES-like (middle) and ES cells (right) are strongly positive.

(D) RT-PCR analysis. Three-fold serial dilutions of cDNA from GS, ES-like, and ES cells were amplified with specific primers. Scale bar, 200 μm.

cells from p53 KO mice had an androgenetic imprint pattern. However, a loss of methylation in the DMRs of *H19*, *Meg 3/G*, and *Rasgrf1* regions and methylation of the DMRs in the *Igf2r* region were observed immediately after the appearance of ES-like cells. The perturbation of imprint patterns continued even when GS cells disappeared, and only the DMR of the *Peg10* region was intact, 18 days after the appearance of ES-like cells. DMR of *Oct-4* region in ES and ES-like cells were all hypomethylated, which confirms their undifferentiated state (Hattori et al., 2004) (Figure 3C).

Differentiation Potential of ES-Like Cells In Vitro and In Vivo

To determine whether ES-like cells can differentiate into somatic cell lineages, we used methods designed to induce differentiation of ES cells in vitro. ES-like cells were first transferred to an OP9 stromal feeder layer, which can support differentiation of mesodermal cells such as hematopoietic or muscle cells (Nakano et al., 1994; Schroeder et al., 2003). Within 10 days, a variety of cell types were identified including hematopoietic cells, vascular cells, and spontaneously beating myocytes (Figures 4A–4H). Hematopoiesis could also be induced when ES-like cells were cultured in methylcellulose to form embryoid bodies (Figure 4I). When we transferred ES-like cells onto gelatin-coated dishes for the differentiation of neural-lineage cells (Ying et al., 2003), they formed neurons or glial cells (Figures 4J–4L). Dopaminergic neurons were also found, albeit at low frequency (Figure 4M). When we compared the differentiation efficiency using ES cells, ES-like cells produced more glial cells than did ES cells, and there were significantly more vessel or heart muscle cell colonies from ES-like cells. However, ES-like cells could produce all of the expected lineages using protocols for ES cell differentiation (Table 1).

ES-like cells were further examined for their ability to form teratomas in vivo by subcutaneous injection into nude mice. Transplanted cells gave rise to typical teratomas in all recipients (eight of eight) by 4 weeks after transplantation (Figure 4N). The tumors contained deriv-

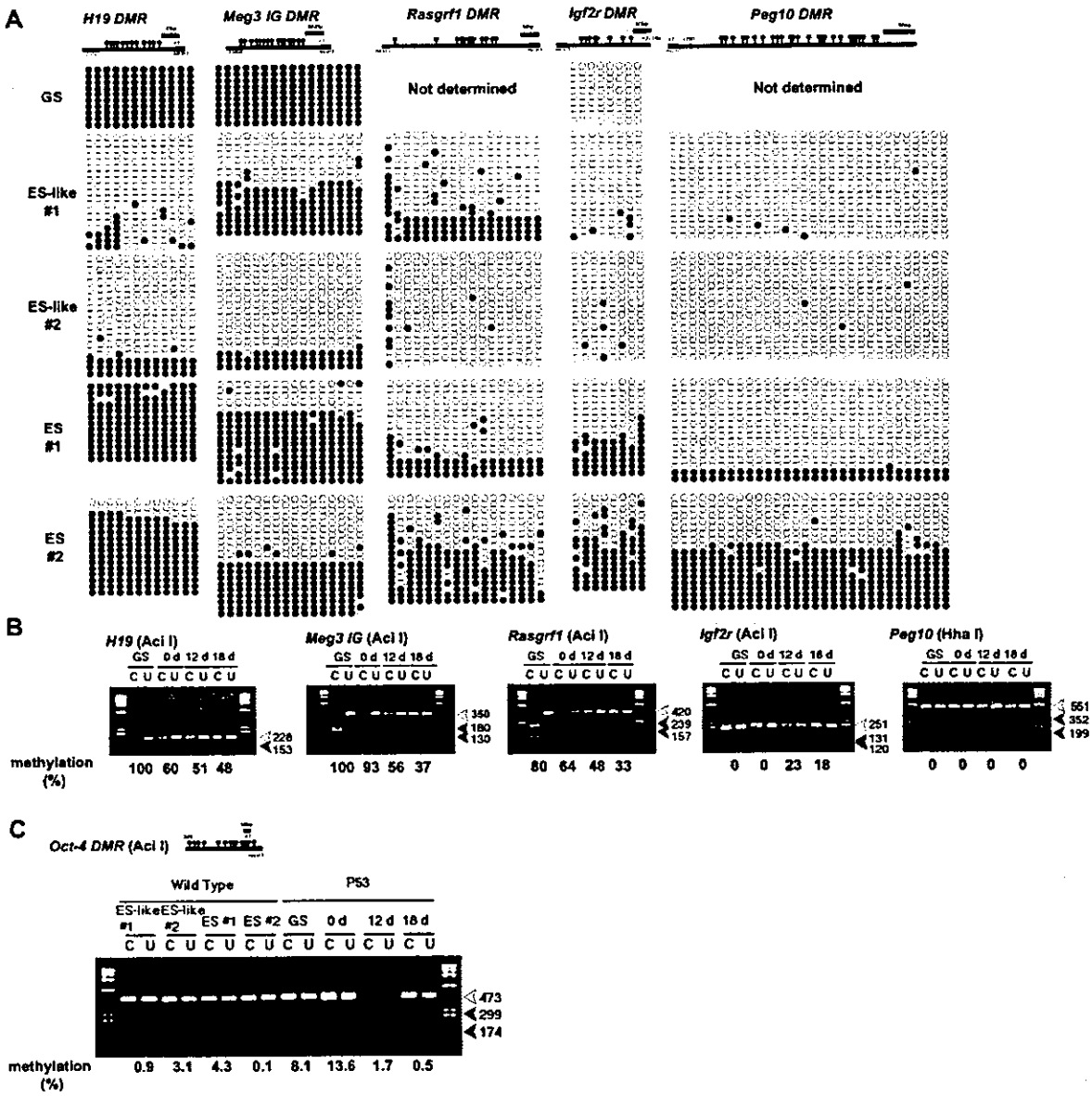

Figure 3. Analysis of Imprinting in ES-Like Cells

(A) DMR methylation of *H19*, *Meg3 IG*, *Rasgrf1*, *Igf2r*, and *Peg10* regions. DNA methylation was analyzed by bisulfite genomic sequencing. Black ovals indicate methylated cytosine-guanine sites (CpGs), and white ovals indicate unmethylated CpGs.

(B) COBRA of GS and ES-like cells from p53 knockout mice. The day when ES-like colonies were found was designated day 0, and cells were collected at the indicated time. In this culture, only ES-like cells were found by day 12.

(C) COBRA of *Oct-4* gene upstream region. Open arrowheads indicate the size of unmethylated DNA. Closed arrowheads indicate the size of methylated DNA. Enzymes used to cleave each locus are indicated in parentheses. U, uncleaved; C, cleaved.

atives of the three embryonic germ layers: squamous cell epithelium, neuroepithelium, and muscle. Similar results were obtained with three different clones or with ES-like cells from p53 knockout mice (eight of eight), and we did not observe a significant histological difference from teratomas derived from ES cells. In contrast, no tumors developed after transplantation of GS cells or fresh testis cells (data not shown).

Since the ES-like cells originated from testis, their ability to differentiate into germline cells was examined using the spermatogonial transplantation technique (Brinster and Zimmermann, 1994). This method allows spermatogonial stem cells to recolonize the empty seminiferous tubules of infertile animals and differentiate into mature sperm. We transplanted the cultured cells into immune-suppressed immature W mice (Kanatsu-Shinohara et al., 2003b). These mice are congenitally infertile and have no differentiating germ cells (Brinster and Zimmermann, 1994). One month after transplantation, all recipient animals (ten of ten) developed teratomas in

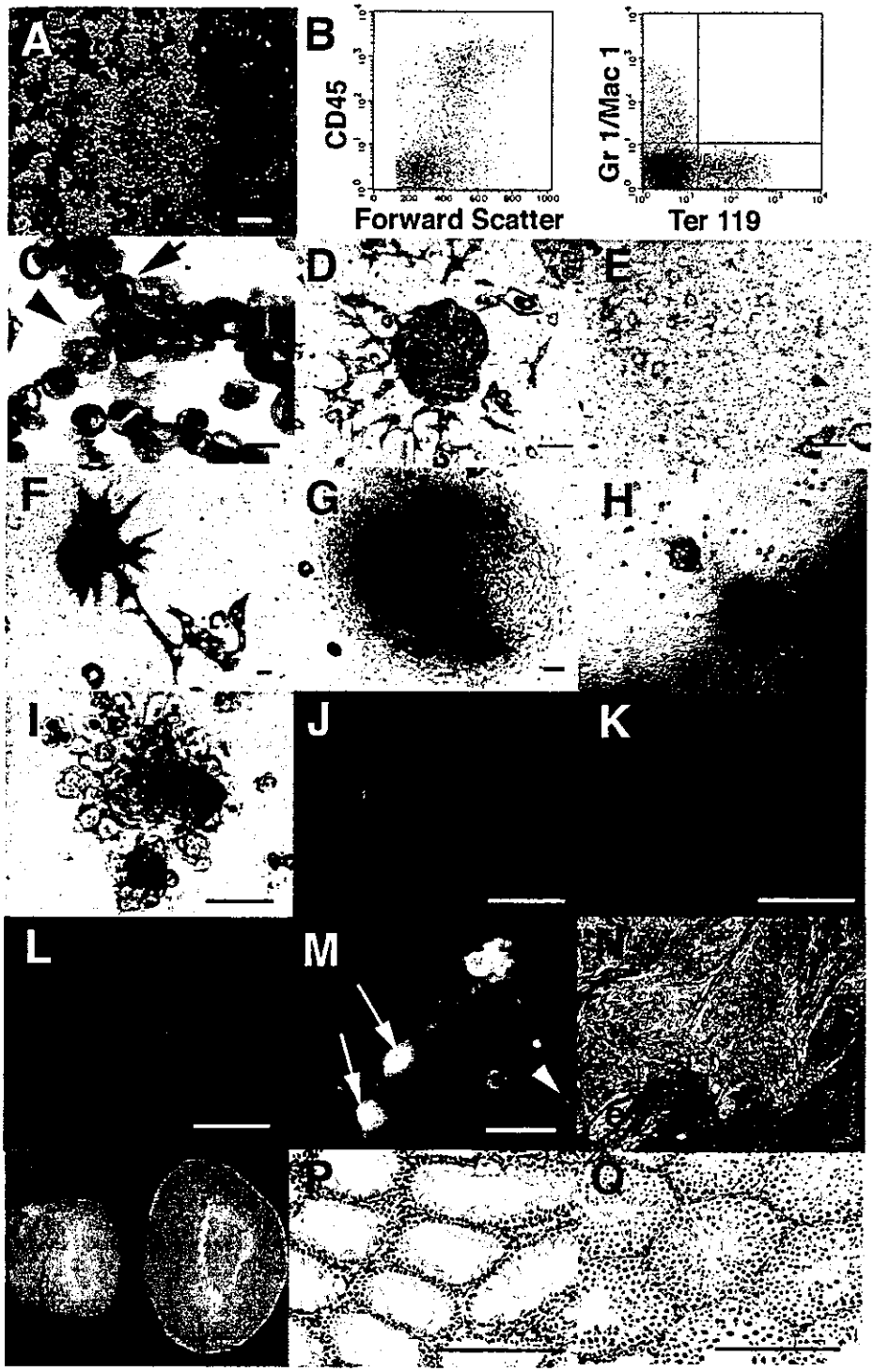

Figure 4. In Vitro and In Vivo Differentiation of ES-Like Cells

(A–H) Differentiation on OP9 cells. (A) Cobblestone formation on day 8. (B) CD45-positive hematopoietic cell development on day 7 after coculture (left). In this cell population, Gr1-positive granulocytes, Mac1-positive macrophages, or Ter119-positive erythrocytes were found (right). (C) May-Giemsa staining of harvested cells. Myeloid progenitor (arrowhead) and erythroblast (arrow) were observed. (D and E) Vascular cell differentiation. Flk-1-positive cells were sorted on day 4 after coculture, and CD31-positive (D) or VE-cadherin-positive (E) vascular cells appeared at 6 days after cell sorting. (F–H) Heart muscle differentiation. The Flk-1-positive cells were differentiated into MF20-positive (F) or cTn-I-positive (G) heart muscle at 6 days after sorting. (H) ANP-positive (blue) atrial muscle and MLC2v-positive (brown) ventricular muscle.
(I) Erythroid cells that developed from embryoid body in methylcellulose at 8 days after culture. Note the red color of the cells.
(J–M) Neuronal cell differentiation on gelatin-coated plates. Tuj-positive neurons (J) on day 5, GFAP-positive astrocytes (K) and MBP-positive

Table 1. In Vitro Differentiation of ES-Like Cells from Testis

	Hematopoiesis[a,b]			Vasculogenesis[a,c]		Neurogenesis[d]		
Cell type	Increase in cell number (fold)	Granulocyte/ Macrophage (%)	Erythrocyte* (%)	Vessel*	Heart*	Neuron*	Astrocyte*	Oligodendrocyte*
ES-like	116.7 ± 15.4	7.6 ± 0.2	19.9 ± 0.7	111.5 ± 12.0	8.0 ± 4.5	126.7 ± 14.4	34.6 ± 4.4	4.6 ± 2.5
ES cell	102.3 ± 11.6	7.6 ± 0.4	24.7 ± 0.9	49.0 ± 9.2	3.8 ± 2.0	162.2 ± 14.5	10.5 ± 3.3	0.2 ± 0.1

Values are mean ± SEM. Results from at least three experiments. ES cells were derived from 129 mice, whereas ES-like cells were derived from DBA/2 mice.

[a] Flk-1-positive cells (5×10^3) were sorted 4 days after coculture and replated on OP9 feeder in a 24-well plate.

[b] Cells were recovered 7 days after sorting and analyzed by flow cytometry. Erythrocytes, macrophages, and granulocytes were identified by anti-Ter119, anti-Mac1, and anti-Gr1 antibodies, respectively.

[c] Numbers of positive cells in each well, 8 days after sorting. Vascular cells were determined by the uptake of DiI-acetylated low-density lipoprotein. Heart muscle colonies were identified by counting beating colonies.

[d] Cells (2.5×10^4) were plated on gelatin in a 48-well plate, and numbers of positive cells per cm^2 were determined by immunocytochemistry 5 (neuron) or 7 (astrocytes or oligodendrocytes) days after plating. Neurons were identified by anti-Tuj antibody, whereas astrocytes and oligodendrocytes were identified by anti-GFAP or anti-MBP antibodies, respectively. Dopaminergic neurons were produced ~10 cells per well.

* Statistically significant by Student's t test ($p < 0.05$).

the testis. The seminiferous tubules were disorganized, and no sign of spermatogenesis was found in histological sections. The cell composition found in the teratomas was similar to that of tumors that developed after subcutaneous injection (data not shown). In contrast, both wild-type and p53 KO GS cells produced normal spermatogenesis when transplanted into the seminiferous tubules (Figures 4O–4Q).

Contribution of ES-Like Cells to Normal Embryonic Development after Blastocyst Injection

Finally, we microinjected ES-like cells into blastocysts to examine whether they can contribute to chimeras in vivo. Five to fifteen cells were injected into C57BL/6 blastocysts. The ratio of euploid cells, which significantly influences the rate of chimerism or germline transmission (Longo et al., 1997; Liu et al., 1997), was 70% at the time of injection.

Some of the recipient animals were analyzed at 12.5 dpc to look for chimerism, and others were allowed to develop to term. Chimerism was observed in 25% (three of 12) of the 12.5 dpc embryos (Figure 5A) and in 36% (13 of 36) of the newborn animals (Figure 5B), as judged by the expression of EGFP observable under UV illumination. Chimerism was also confirmed by the coat color at mature stage (Figure 5C). We found six dead fetuses that showed EGFP expression, and some embryos were partially or completely absorbed. The pattern of contribution was similar at both stages analyzed; EGFP-positive donor cells were found in the central nervous system, liver, heart, lung, somites, intestine, and other tissues, including the yolk sac and chorionic membrane of the placenta (Figures 5D–5I).

Since donor cells were also found in the testis of a chimeric animal at 6 weeks of age (Figure 5J), we performed microinsemination to obtain offspring. Round spermatids were collected and microinjected into C57BL/6 × DBA/2 (BDF1) oocytes. Of 81 cultured embryos, 64 (79%) developed into 2-cells and were transferred into five psudopregnant females. Eighteen (22%) embryos were implanted, and one of the two offspring from a recipient mouse showed EGFP fluorescence, indicating the donor origin (Figure 5K). Interestingly, while control ES cells showed wide contribution to embryos, no donor cell contribution was observed in experiments using GS cells (Table 2).

To determine the full developmental potential of ES-like cells, we used tetraploid complementation technique (Nagy et al., 1993). This technique allows the production of live animals that consist entirely of donor ES cells. A total of 92 tetraploid embryos were created by electrofusion, aggregated with ES-like cells, and transferred to pseudopregnant ICR females. When some of the recipient animals were sacrificed at 10.5 dpc, we found one normal-looking fetus and several resorptions with normal placentas. The fetus showed some growth retardation but clearly expressed the EGFP gene throughout its body, including the yolk sac (Figure 5L), indicating that it was derived from donor ES-like cells. However, none of the pseudopregnant mothers sired live offspring from both ES-like and ES cells.

Discussion

The results of our experiments revealed the presence of multipotential stem cells in the neonatal testis. Although some cases of the "stem cell plasticity" phenomenon

oligodendrocytes (L) on day 7 after induction. TH and Tuj-double positive dopaminergic neurons (arrow) appeared among Tuj-positive neurons (arrowhead) (M).

(N) Section of a teratoma under the skin. The tumors contained a variety of differentiated cell types, including muscle (m), neural (n), and epithelial (e) tissues.

(O–Q) Spermatogenesis from p53 knockout GS cells. (O) A macroscopic comparison of untransplanted (left) and transplanted (right) recipient testes. Note the increased size of the transplanted testis. (P and Q) Histological appearance of the untransplanted (P) and transplanted (Q) W testes. Note the normal appearance of spermatogenesis (Q). Color staining: Cy3, red (J–M); Alexa Fluor 488, green (M). Scale bar, 50 μm (A, D–I, J, K, and M), 20 μm (C and L), 200 μm (N, P, and Q), 1 mm (O).

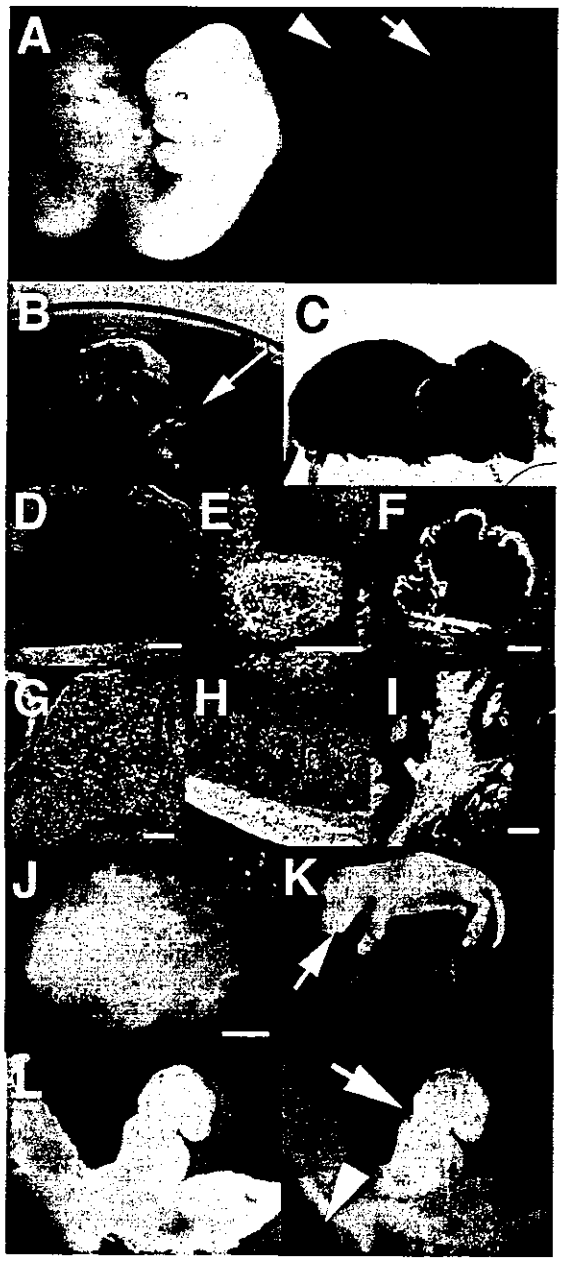

Figure 5. Production of Chimeric Animals

(A) A 12.5 dpc chimeric embryo (arrow) showing fluorescence under UV light. No fluorescence was observed in a control embryo (arrowhead).

(B) A newborn chimeric animal (arrow) showing fluorescence.

(C) Mature chimeric animals. Note the donor cell-derived coat color (cinnamon).

(D–I) Parasagittal section of a 12.5 dpc chimeric embryo. Fluorescence was observed in the brain (D), intestine (E), heart (F), liver (G), lower spinal cord (H), and placenta (I).

(J) A testis from a chimeric mouse showing fluorescence. EGFP expression was observed in some germ cells in the testis cell suspension (inset).

(K) Offspring derived from a chimera. One of the offspring showed fluorescence, confirming the donor origin (arrow).

(L) A 10.5 dpc embryo (arrow) and yolk sac produced from an aggregation of ES-like cells with tetraploid embryo showing fluorescence. No fluorescence was observed in the placenta (arrowhead). Counterstained with propidium iodide (PI) (D–I). Color staining: EGFP, green (A, B, and D–L); PI, red (D–I). Scale bar, 100 μm (D–I), 1 mm (J).

have been attributed to cell fusion (Wagers and Weissman, 2004), our case cannot be explained by the same mechanism because the ES-like cells formed teratomas after subcutaneous transplantation. These ES-like cells from the testis can be considered the neonatal counterparts of ES/EG cells. The result was unexpected, since PGCs become resistant to experimental teratocarcinogenesis or EG cell formation after 13.5 dpc (Stevens, 1984; Labosky et al., 1994). To our knowledge, EG cells are the only example of the isolation of multipotent stem cells from primary germ cells (Resnick et al., 1992; Matsui et al., 1992). EG cells were derived from primary germ cells harvested from 8.5 to 12.5 dpc fetuses and cultured in vitro with a mixture of mSCF, LIF, and bFGF. However, pluripotent cells could not be isolated from neonatal germ cells using the same culture conditions (Labosky et al., 1994), except when cells from teratomas were used (Robertson and Bradley, 1986). ES-like cells are unlikely to be derived from teratoma cells for two reasons. First, the frequency of derivation of ES-like cells in our study was significantly higher than the negligible rate of spontaneous teratoma formation in strains other than 129 and A/He mice (one teratoma out of 11,292 males in 129 hybrid backgrounds) (Stevens and Mackensen, 1961). Second, growth factor supplementation was essential for the establishment of ES-like cells. In fact, few EC cell lines have been obtained from spontaneously occurring teratocarcinomas (Robertson and Bradley, 1986). These findings strongly suggest that the ability to become multipotent stem cells persists in neonatal testis. Based on the results reported here, we propose to name these ES-like cells multipotent germline stem cells, or mGS cells, to distinguish them from GS cells, which can differentiate only into germline cells (Kanatsu-Shinohara et al., 2003a).

An important question that arises from this study is the origin of mGS cells. One possibility is that they appear independently from GS cells and originate from a population of undifferentiated pluripotent cells that persist in the testis from the fetal stage. Although EG cells have been established from ~12.5 dpc PGCs (Matsui et al., 1992; Labosky et al., 1994), cells with similar characteristics might remain in neonatal testis and produce ES-like cells. Indeed, the results of the imprinting analysis of wild-type mGS cells suggest a distinct origin for mGS cells. In male germ cells, genomic imprinting is erased during the fetal stage, and male-specific imprinting begins to be acquired around birth in prospermatogonia and is completed after birth (Davis et al., 1999, 2000; Kafri et al., 1992). While GS cells had a typical androgenetic imprinting pattern, the imprinting pattern of mGS cells clearly differed from those of androgenetic germ cells or somatic cells, which suggested that mGS cells originate from partially androgenetic germ cells that have undergone imprint erasure.

Another possibility is that mGS cells are derived from spermatogonial stem cells and that the ability to become multipotential cells may be one of the general character-